Adenosine A_1 Receptor mRNA Expression by Neurons and Glia in the Auditory Forebrain

TROY A. HACKETT *

[1]Department of Hearing and Speech Sciences, Vanderbilt University Medical Center, Nashville, Tennessee, USA
[2]Department of Psychology, Vanderbilt University, Nashville, Tennessee, USA
[3]Vanderbilt Brain Institute, Vanderbilt University, Nashville, Tennessee, USA
[4]Vanderbilt Kennedy Center for Research on Human Development, Vanderbilt University, Nashville, Tennessee, USA

ABSTRACT

In the brain, purines such as ATP and adenosine can function as neurotransmitters and co-transmitters, or serve as signals in neuron–glial interactions. In thalamocortical (TC) projections to sensory cortex, adenosine functions as a negative regulator of glutamate release *via* activation of the presynaptic adenosine A1 receptor (A_1R). In the auditory forebrain, restriction of A_1R-adenosine signaling in medial geniculate (MG) neurons is sufficient to extend LTP, LTD, and tonotopic map plasticity in adult mice for months beyond the critical period. Interfering with adenosine signaling in primary auditory cortex (A1) does not contribute to these forms of plasticity, suggesting regional differences in the roles of A_1R-mediated adenosine signaling in the forebrain. To advance understanding of the circuitry, *in situ* hybridization was used to localize neuronal and glial cell types in the auditory forebrain that express A_1R transcripts (*Adora1*), based on co-expression with cell-specific markers for neuronal and glial subtypes. In A1, *Adora1* transcripts were concentrated in L3/4 and L6 of glutamatergic neurons. Subpopulations of GABAergic neurons, astrocytes, oligodendrocytes, and microglia expressed lower levels of *Adora1*. In MG, *Adora1* was expressed by glutamatergic neurons in all divisions, and subpopulations of all glial classes. The collective findings imply that A_1R-mediated signaling broadly extends to all subdivisions of auditory cortex and MG. Selective expression by neuronal and glial subpopulations suggests that experimental manipulations of A_1R-adenosine signaling could impact several cell types, depending on their location. Strategies to target *Adora1* in specific

ABBREVIATIONS: A1 = primary auditory cortex; A_1R = adenosine 1a receptor; ADK = adenosine kinase; ADO = adenosine; ADP = adenosine diphosphate; AMP = adenosine monophosphate; Aqp4 = aquaporin-4; ATP = adenosine triphosphate; AuD/AuV = dorsal/ventral auditory areas; CA1/CA3/DG = hippocampus subdivisons; CC = corticocortical projection; Ct = corticotectal projection; CT = corticothalamic projection; d = dorsal division (of MG); ENase = ectonucleotidase; Ent = entorhinal cortex; ENT = equilibrative nucleoside transporter; Gapdh = glyceraldehyde 3-phosphate dehydrogenase; Hip = hippocampus; Itgam = integrin subunit alpha M; m = medial division (of MG); MBP = myelin basic protein; MG = medial geniculate body; mz = marginal zone (of MGv); Nt5E = ecto-5′-nucleotidase (CD73); PG = pontine gray; Pil = peri interlaminar n.; PP = peripeduncular n.; RS = retrosplenial area; SC = superior colliculus; TC = thalamocortical projection; v = ventral division (of MG); VGAT = vesicular GABA transporter; VGluT1 = vesicular glutamate transporter 1; VGluT2 = vesicular glutamate transporter 2; wm = white matter

Grant sponsor: National Institutes of Health (NIH); Grant number: R01 DC015388; Grant sponsor: National Institute on Deafness and Other Communication Disorders (NIDCD).

*Correspondence to: Troy A. Hackett, Ph.D., Professor of Hearing and Speech Sciences, Vanderbilt University Medical Center, 465 21 Avenue South, MRB-3 Suite 7114, Nashville, TN 37240. E-mail: troy.a.hackett@vanderbilt.edu

Received 24 July 2017; Revised 5 December 2017; Accepted 10 January 2018.

DOI: 10.1002/ar.23907
Published online 12 October 2018 in Wiley Online Library (wileyonlinelibrary.com).

cell types can be developed from the data generated here. Anat Rec, 301:1882–1905, 2018. © 2018 The Authors. *The Anatomical Record* published by Wiley Periodicals, Inc. on behalf of American Association of Anatomists.

Key words: cortex; thalamus; medial geniculate; purine; neurotransmission; plasticity

1. INTRODUCTION

Purines and pyrimidines are nucleotides found in all cells, contributing to multiple processes, such as DNA/RNA construction, energy homeostasis, and cell signaling. In the peripheral and central nervous systems, purinergic signaling is a widespread mechanism for communication between neurons, glia, and vascular cells. Purines such as adenosine and adenosine triphosphate (ATP) can function as neurotransmitters, co-transmitters, neuromodulators, and as signals in neuro–glial interactions (Burnstock, 2007; Boison, 2008a; Abbracchio et al., 2009; Housley et al., 2009; Koles et al., 2016). Accordingly, their functional impact on the nervous system is broad, including key roles in development, behavior, regeneration, plasticity, and pathology (Dale, 2008; Burnstock et al., 2011; Wei et al., 2011; Zimmermann, 2011; Del Puerto et al., 2013; Dias et al., 2013; Sebastiao and Ribeiro, 2015; Krugel, 2016; Pedata et al., 2016). In the brain, ATP and adenosine are released in an activity dependent manner from the presynaptic terminals of neurons by vesicle-mediated exocytosis, postsynaptic membranes (dendrites), and axons (Fredholm et al., 2005; Wall and Dale, 2008; Abbracchio et al., 2009; Burnstock et al., 2011; Cunha, 2016). They may also be released by glia, especially astrocytes, *via* vesicular secretion, transport proteins, and membrane channels (Boison et al., 2010; Koles et al., 2016).

Their actions are mediated by purinergic receptors at pre-, post-, and nonsynaptic sites on neurons and glia. Adenosine is bound by members of the P1 receptor class (G-protein-coupled), and ATP by the larger P2 receptor family (P2X, ligand-gated ion channel; P2Y, G-protein-coupled). The P1 and P2 receptor subtypes have varied levels of expression in neurons and glia of the cortex, hippocampus, cerebellum, striatum thalamus, brainstem, and spinal cord (Fields and Burnstock, 2006; Wei et al., 2011). For the P1 class, distributions of its four subtypes (A_1, A_{2A}, A_{2B}, and A_3) are generally distinct, with overlap in some brain regions, and may be colocalized in some cells. Likewise, the P2 receptors are widely expressed by neurons and glia in the brain, where the localization of specific subtypes can be distinct (Burnstock and Knight, 2004). Cell type-specific transcriptome profiling has revealed that the expression of P1 and P2 receptors differs substantially among several major neuronal and glial subtypes (Cahoy et al., 2008; Zhang et al., 2014; Zeisel et al., 2015). In the auditory forebrain, transcriptome profiling indicated that several members of the P1 and P2 receptor classes are expressed in A1 and MG (Hackett et al., 2015). P1-class expression was dominated by the A_1 subtype, and P2-class expression was highest for *P2rx4*, *P2rx7, P2ry1,* and *P2ry12* (Fig. 1). Additionally, transcript levels tended to increase or decrease during the maturational period studied (P7 through adult), especially between P7 and P14 (before and after hearing onset).

Studies in hippocampus and other brain regions reveal that adenosine can regulate synaptic transmission and plasticity through A_1 and A_{2a} receptors located at pre- and postsynaptic sites on neurons and astrocytes (Ochiishi et al., 1999; Rebola et al., 2005; Sebastiao and Ribeiro, 2009; Sperlagh and Vizi, 2011; Ota et al., 2013; Chen et al., 2014; Sebastiao and Ribeiro, 2015). Importantly, neuromodulation by adenosine is not limited to glutamatergic transmission, but also other modulators (e.g., GABA, acetylcholine, BDNF, cannabinoids). The actions of adenosine *via* A_1 and A_{2a} receptors are most often associated with inhibition and facilitation, respectively. The inhibitory effects of A_1 receptors have primarily been observed at glutamatergic and cholinergic

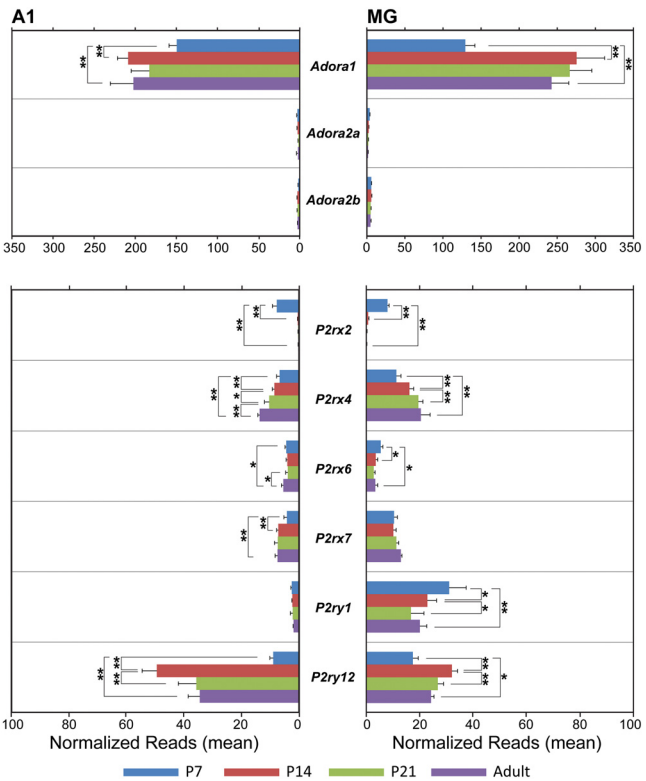

Fig. 1. Purinergic receptor transcript expression in the auditory forebrain (A1, MG) during postnatal development. For each gene, mean normalized read counts derived from RNA sequencing of A1 and MG are plotted at 4 postnatal ages (P7, P14, P21, adult). *Adora1* expression (top panels) is plotted separately from the P2 receptors (bottom panels) due to differences in scale. $^*P < 0.05$; $^{**}P < 0.01$. Data derived from Hackett et al. (2015) database.

endings (hippocampus), but not GABAergic (Cunha and Ribeiro, 2000; Cristovao-Ferreira et al., 2009). Instead, the A_1 receptor appears to have indirect influence in particular interneuron subpopulations (Klausberger et al., 2005; Rombo et al., 2016), indicating cell-type specificity in expression (Rivkees et al., 1995; Ochiishi et al., 1999) and mechanisms of action.

Consistent with the foregoing, recent studies of thalamocortical (TC) inputs to sensory cortex have revealed that adenosine functions as a negative regulator of glutamate release *via* activation of presynaptic A_1 receptors (Fontanez and Porter, 2006; Bayazitov et al., 2007; Blundon et al., 2011; Chun et al., 2013; Ferrati et al., 2016). In the auditory forebrain, restriction of A_1-mediated adenosine signaling in medial geniculate (MG) neurons is sufficient to extend LTP, LTD, and tonotopic map plasticity in adult mice for months beyond the critical period (Blundon et al., 2011; Chun et al., 2013; Blundon et al., 2017). In contrast, restricting adenosine signaling in neurons of the primary auditory cortex (A1) does not contribute to these forms of plasticity, suggesting that the effects are confined to presynaptic TC projections. Thus, adenosine signaling through presynaptic A_1 receptors on TC terminals appears to act as a gate that regulates glutamate release and plasticity at TC synapses in A1.

1.1 *Adora1* Expression by Neurons and Glia in the Auditory Forebrain

The focus of this study is the adenosine A_1 receptor subtype (hereafter, A_1R). The purpose was to advance understanding of the circuitry involved in A_1R-mediated adenosine signaling in the auditory forebrain by cells that express A_1R mRNA transcripts (i.e., *Adora1*). Specific goals were to identify the neuronal and glial cell subtypes that express *Adora1*, and map their locations across laminae in primary auditory cortex (A1) and nuclear subdivisions of the medial geniculate body (MG), based on co-expression with cell-type specific markers.

Rationale for this study includes several observations. First, as indicated above, adenosine receptor expression is widespread, but can vary by brain region, cell class, and receptor subtype. The A_1R subtype is the most highly expressed purinergic receptor in the auditory forebrain (Fig. 1), but its regional- and cell-type-specificity have not been profiled. Thus, the structural foundation for studies of A_1R function has not been established.

Second, glia and neuron–glia interactions are involved in a vast array of brain functions that often involve adenosine signaling (Stevens et al., 2002; Fields and Burnstock, 2006; Boison, 2008a; Pelligrino et al., 2011; Lovatt et al., 2012; Del Puerto et al., 2013; Domercq et al., 2013; Bynoe et al., 2015; Coppi et al., 2015; Koles et al., 2016). Whether *Adora1* expression is restricted to specific neuronal and glial subpopulations or subdivisions of the auditory forebrain is unknown, but this knowledge is essential for the understanding and modeling of adenosine signaling in forebrain circuits.

Third, cell-specific expression patterns have important implications for the design of experimental studies expecting to target *Adora1* (e.g., optogenetics, gene editing, pharmacology, behavior). Target specificity can significantly impact experimental outcomes and must be incorporated into experimental designs. For example, altering A_1R expression at the mRNA or protein levels would be expected to produce different results if expression was common to all cells, as opposed to particular neuronal or glial subpopulations.

With these goals in mind, *in situ* hybridization (ISH) was used to profile the expression of *Adora1* transcripts in subclasses of neurons (glutamatergic, GABAergic) and glia (astrocytes, oligodendrocytes, microglia) in the auditory forebrain of adult mice. The results indicate that *Adora1* is widely expressed by neurons and glia in A1 and MG, but in a manner that varies by cell type and specific location. Thus, A_1R-mediated adenosine signaling would be expected to differentially impact subpopulations of neurons and glia in the auditory forebrain. Strategies to target *Adora1* in specific cell types can be developed from the data generated here.

2. MATERIALS AND METHODS

2.1 Tissue Acquisition

All procedures were approved by the Animal Care and Use Committee at Vanderbilt University and followed the guidelines established by the National Institutes of Health for the care and use of laboratory animals. Brains collected from adult (8–10 weeks) C57BL/6J mice (Jackson Labs 000664), 8 of each sex. Animals were anesthetized with isoflurane in an isolation chamber until areflexive, and decapitated. Brains were immediately removed, blocked in the coronal plane, embedded in OCT compound (Tissue-Tek, Torrance, CA), then flash frozen in liquid-nitrogen-cooled isopentane. Blocks containing 4 brains each (2 male and 2 female) were stored at −80°C. Blocks were sectioned coronally at 10 μm, and collected onto Superfrost Plus slides (Thermo Fisher Scientific, Waltham, MA), and stored at −80°C prior to histological assays.

2.2 Selection of Neuronal and Glial Markers

Adora1 mRNA expression was studied in three subtypes of neurons and glia, based on co-expression for cell-specific markers (Table 1). Subpopulations of glutamatergic neurons were distinguished by expression or co-expression of vesicular glutamate transporters 1 and 2 (*VGluT1, VGluT2*), which have a partially complementary distribution in the brain (Kaneko and Fujiyama, 2002; Fremeau et al., 2004). The expression of the vesicular GABA/glycine transporter (*VGAT*) is specific to GABAergic and glycinergic neurons (Chaudhry et al., 1998; Dumoulin et al., 1999). In a prior study, we mapped the spatial distributions of glutamatergic and GABAergic neurons in A1 and MG of adult and developing mice, based on expression of these markers (Hackett et al., 2016). *VGluT1* was preferentially expressed in A1, and *VGluT2* was co-expressed with *VGluT1* in a small subset of those neurons. In MG, nearly all neurons expressed *VGluT2* or co-expressed *VGluT1* and *VGluT2*. The expression of *VGAT* was restricted to neurons in A1, as GABAergic neurons are rare in the rodent MG. The *VGluT1, VGluT2,* and *VGAT* transcripts are highly specific to glutamatergic and GABAergic neuronal subpopulations in the forebrain (Zeisel et al., 2015).

Glial cell distributions have not been previously mapped in the auditory forebrain. Markers of each glial class were selected to achieve specific expression for that cell type, as well as the broadest expression across

TABLE 1. Details of riboprobes for *Adora1* and markers of neuronal and glial subtypes targeted by *in situ* hybridization

Cell type	Protein	Gene	Accession No.	Position
Glutamatergic neuron	Vesicular glutamate transporter 1	*Slc17a7 (VGluT1)*	NM_182993.2	464–1,415
Glutamatergic neuron	Vesicular glutamate transporter 2	*Slc17a6 (VGluT2)*	NM_080853.3	1986–2,998
GABAergic neuron	Vesicular GABA/glycine transporter	*Slc32a1 (VGAT)*	NM_009508.2	894–2037
Astrocyte	Aquaporin-4	*Aqp4*	NM_009700.2	1,646–2,644
Oligodendrocyte	Myelin basic protein	*MBP*	NM_001025259.2	648–2,107
Microglia	Integrin subunit Alpha M	*Itgam (Cd11b)*	NM_001082960.1	538–1,528
General marker, positive control	Glyceraldehyde 3-phosphate dehydrogenase	*Gapdh*	NM_008084.2	21–935
All	Adenosine A1 receptor	*Adora1*	NM_001008533.2	4,018–4,999

subpopulations of each class. For myelinating oligodendrocytes, myelin basic protein (*MBP*) was chosen for ubiquitous expression in myelinating oligodendrocytes in mature animals (Cahoy et al., 2008; Zeisel et al., 2015; Holt and Olsen, 2016). For astrocytes, aquaporin-4 (*Aqp4*) was chosen over the more commonly used marker, glial fibrillary astrocytic protein (*GFAP*). *Aqp4* is highly specific to astrocytes (Venero et al., 1999; Badaut et al., 2002; Nicchia et al., 2004; Saadoun et al., 2005; Hsu et al., 2011; Aoyama et al., 2012; Papadopoulos and Verkman, 2013; Smith et al., 2014; Hubbard et al., 2015), and transcript expression levels are higher than *GFAP* for both major astrocyte subtypes (Cahoy et al., 2008; Zhang et al., 2014; Zeisel et al., 2015). Some evidence also suggests that *GFAP* is nominally expressed by some astrocyte subpopulations (Cahoy et al., 2008; Zeisel et al., 2015), and may be co-expressed with chondroitin sulfate proteoglycan 4 (aka: *Cspg4*, *NG2*), a marker of oligodendrocyte precursor cells (Zhang et al., 2014; Alghamdi and Fern, 2015). For microglia, several specific markers of microglia are known (e.g., *Aif1, Cx3cr1*, *Hexb, Tlr4*), but the cell adhesion molecule, integrin alpha-M (*Itgam*) (aka *Cd11b*) was chosen because it is more widely used as a marker and expressed by all subtypes (Zhang et al., 2014; Zeisel et al., 2015; Holt and Olsen, 2016).

2.3 *In situ* Hybridization (ISH)

Chromogenic and multiplex fluorescence assays were conducted using custom riboprobes designed and manufactured by Advanced Cell Diagnostics (ACD, Hayward, CA) (Wang et al., 2012) (Table 1). The vesicular transporter probes were previously used in studies of the mouse auditory forebrain (Hackett et al., 2016). These proprietary probes and assays (RNAscope) utilize a unique signal amplification and background suppression methodology that consistently yielded exceptionally high sensitivity and specificity with low background. Briefly, after a 30-min protease permeabilization step, two independent probes (double Z probe) were hybridized for 2 hr to each target sequence (~20 probe pairs per target molecule). The lower region of each probe is complementary to the target sequence, and the upper region is a 14-base tail sequence. Together, the dual probe construct provides a 28-base binding site for the preamplifiers, which were built up during a multistage amplification cycle. In the final steps, labeled probes containing the fluorescent or chromogen conjugates were bound to each of the 20 binding sites on each preamplifier. All incubation steps were performed at 40°C in a hybridization oven (HybEZ, ACD, Hayward CA) using the RNAscope Multiplex Fluorescent or Duplex Reagent kits, according to the manufacturer's instructions for fresh frozen brain tissue.

Single colorimetric ISH assays were conducted for *Adora1*, *VGluT1*, *VGluT2*, *VGAT*, *MBP*, *Aqp4*, and *Itgam* as a baseline reference for the locations of labeled cells. Then, duplex chromogenic assays paired each cell marker with the housekeeping gene, *Gapdh* (glyceraldehyde-3-phosphate dehydrogenase) as a positive control for a second riboprobe. Additional series of duplex chromogenic assays paired each cell marker with *Adora1*. In duplex assays, the red and blue–green substrates were fast-red and fast-green, respectively. As a negative control, sections were incubated in buffer solution that did not contain any riboprobes. These assays revealed no significant labeling in any channel. Multiplex fluorescence ISH (FISH) was performed in two separate series of sections. One combined all three neuronal markers with *Adora1* in separate channels (*VGluT1*, *VGluT2*, *VGAT*, *Adora1*), the other combined all three glial markers with *Adora1* (*MBP*, *Aqp4*, *Itgam, Adora1*). These assays were done to permit visualization of all genes in a single tissue section, and as a positive control for marker specificity.

All sections were counterstained to improve identification of brain areas and provide a focal point for cytoplasmic probe labeling. FISH-reacted sections were counterstained with DAPI (30 sec), and chromogen-reacted sections were counterstained with 50% hematoxylin (30 sec).

2.4 Antibody Selection and Immunohistochemistry (IHC)

Four commercially available primary antibodies for A_1R were evaluated for staining quality and consistency (Table 2). Antibody specificity was tested by incubating each antibody with a 10× concentration of the control protein provided by the manufacturer, when available. Negative controls, omitting the primary antibody, were used in the testing of all antibodies to assess nonspecific staining. Optimal primary antibody concentrations were determined from these tests, as listed in Table 2. The Protein-Tech antibody consistently produced the strongest punctate signals in chromogenic assays of fresh frozen and fixed tissues. This A_1R antibody was combined with the neuron-specific marker, NeuN (*Fox3*) in dual fluorescence IHC assays as a marker of neuronal nuclei and somata, as detailed previously (Hackett et al., 2016). Secondary antibodies used for IHC and FIHC are listed in Table 2.

TABLE 2. Primary and secondary antibodies used for IHC

Antibody	*Species*	*Supplier*	*Part Number*	*Dilution*	*References*
Primary antibodies					
Adora1 A_1R	rb	Protein-Tech	55,026-1-AP	1:250	Burke et al., 2015
Adora1 A_1R	rb	Novus Biologicals	NB300-549 RRID:AB_10002337	1:250	Kimura et al., 2003; Yamaguchi et al., 2014
Adora1 A_1R	gp	Alamone Labs	AAR-006 RRID:AB_2039705	1:250	Garcia et al., 2013; Vindeirinho et al., 2013
Adora1 A_1R	rb	Aviva Systems	OABF01723 RRID: not listed	1:250	---
Fox3/NeuN	ms	Covance	SIG39860 RRID:AB_11220035	1:1000	Wimmer et al., 2010
Secondary antibodies					
					Primary antibody combination
Anti-rabbit IgG	G-rb	Vector Labs	BA-1000 RRID:AB_2313606	1:200	Adora1 A_1R
Alexa 647	Ch-rb	Lifetech	A21443 RRID:AB_1500685	1:400	Adora1 A_1R
Alexa 750	Ch-ms	Lifetech	A21037 RRID:AB_1500644	1:400	NeuN (Fox3)

Abbreviations: ms, mouse; rb, rabbit; G/g, goat, Ch, chicken.

Single chromogenic IHC and dual fluorescence IHC (FIHC) assays were performed on slide-mounted fresh-frozen sections (10 μm) and fixed floating sections (40 μm). Sections were rinsed for 30 min in 0.01 M PBS-Tx (phosphate buffered saline, 0.1% triton), followed by three changes of 0.01 M PBS for 10 min (standard rinse procedure). In FIHC assays, nonspecific labeling of myelin by fluorescent secondary antibodies was blocked by incubation in IT-Fx (Life Tech) for 60 min at RT, followed by a standard rinse. In IHC and FIHC, sections were incubated for 5 min at RT in a single purified glyocoprotein blocking solution (Superblock, ScyTek Laboratories, Logan, UT), followed by a single rinse in PBS. Superblock reagent reduces nonspecific antibody binding, and was used in lieu of species-specific sera or bovine serum albumin (Evans et al., 1996; Buttini et al., 2002; Turtzo et al., 2014). IHC sections were incubated for 48 hr in primary antibodies at 4°C, 2 hr in the biotinylated secondary antibody at RT, 1 hr in avidin–biotin solution (Vectastain ABC Kit, PK-6100, Vector Laboratories, Burlingame, CA), then 5 min in the chromogen solution (ImmPACT VIP Kit, SK-4605, Vector Laboratories). FIHC sections were then incubated for 48 hr in the primary antibodies at 4°C, then 2 hr in the secondary antibody cocktail (A_1R + NeuN) at RT. Standard rinsing steps were performed between all incubations. All incubations and rinsing steps were performed on a laboratory shaker with constant agitation.

2.5 Image Acquisition and Analyses

Bright-field images of single colorimetric ISH and IHC tissue sections were obtained with a Nikon 80i microscope controlled by Neurolucida 10 software (MBF Bioscience). Fluorescence wide-field images and image montages of FISH and FIHC sections were obtained with a Nikon 90i epiflourescence microscope and Hamamatsu Orca 4.0 CCD camera, controlled by Nikon Elements AR software using 20×, 40×, and 100× objectives. Exposure parameters for each color channel were maintained at the same levels across all samples to standardize signal intensity. Images were assembled into figures using Adobe Illustrator CS6 (Adobe Systems, Inc.). 40× and 100× images were created from z-plane image stacks collapsed to two dimensions, using an Extended Depth of Focus plugin to the Nikon Elements software.

Identification of auditory cortex and medial geniculate was based on previously established architectonic criteria (Hackett et al., 2011a; Hackett et al., 2016), with reference to standard reference atlases (Franklin and Paxinos, 2007; Lein et al., 2007). Laminar density profiles of *Adora1* expression from auditory cortex (areas A1, AuD, AuV) were derived from images of colorimetric ISH sections converted to 8-bit grayscale, then thresholded at 50% using ImageJ software (NIH, nih.gov). Raw grayscale intensity was measured using rectangular selection boxes (1,000 pixel width) from layer 1 (L1) just below the pial boundary through the white matter below L6. The average grayscale intensity value was averaged across 1,000 pixels of each row of pixels separately for A1. The resulting functions were smoothed using a 200-point moving average.

Cell counts were performed manually from A1 and MG in 4 different brains using diffusion interference contrast (DIC) microscopy (40×, 100×) on chromogen-reacted sections. For each marker, a cell was considered positively labeled (e.g., *Adora1*$^+$) if three or more labeled puncta were contained within the somatic cytoplasm (see Discussion for rationale). The average number of labeled and nonlabeled cells was tabulated for each layer of A1 and division of MG, along with their standard deviations. The X–Y locations of each cell were plotted on schematic diagrams of each brain region. The division between MGm and the suprageniculate nucleus (Sg) was approximated in figures, but their cell counts were combined, as definitive borders between the two divisions were ambiguous in these preparations, and because transcript distributions were typically uniform across the region. The difficulties in delineation of Sg in mouse have been noted previously,

(Jones, 2007; Watson et al., 2012), and identification varies across studies (Cruikshank et al., 2001; Anderson et al., 2009; Lu et al., 2009; Anderson and Linden, 2011; Marquez-Legorreta et al., 2016).

3. RESULTS

3.1 Regional and Local Distributions of *Adora1* mRNA

Adora1 mRNA expression was widespread in the adult mouse brain, but concentrations of *Adora1*$^+$ puncta varied by regional and subcellular location. Figure 2A,B shows a coronal section through the auditory forebrain stained for *Adora1* (red) in a single-probe ISH assay, counterstained with hematoxylin (light blue). *Adora1* signal was most conspicuous in middle and deep layers of cerebral cortex, cell-dense domains of the hippocampus, MG, and superior colliculus.

Laminar intensity profiles in A1 and adjacent fields (AuD, AuV) (Fig. 2C–E) highlight the prominent peaks in L6 and secondary peaks centered on L4. Note that L6 peak magnitude was comparable for all three fields, while the L4 peak was higher in A1. Intensity profiles were not measured in MG, where *Adora1* expression was relatively homogeneous across divisions.

In Figures 3 and 4, duplex ISH labeling of *Adora1* (red) and *Gapdh* (green) (positive control) is illustrated at higher magnification to show labeling at the cellular

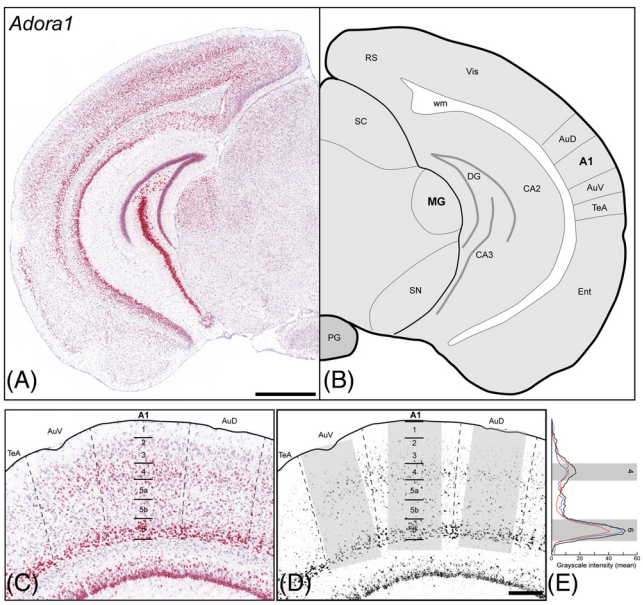

Fig. 2. *Adora1* mRNA expression in a coronal section of the mouse brain at the rostral-caudal level of A1 and MG. **(A)** *Adora1* signal (red) is prominent in the middle and deep layers of cerebral cortex, cellular regions of the hippocampus, MG, superior colliculus (SC), and pontine gray (PG). Hematoxylin counterstain. **(B)** Schematic reference. Scale bar, 1 mm. **(C)** *Adora1* expression across layers of auditory cortex (A1, primary auditory cortex; AuD, dorsal area; AuV, ventral area; TeA, temporal area). **(D)** *Adora1*, 50% thresholded grayscale image from panel C. Gray masked rectangles indicate the portion of each area measured in calculation of grayscale intensity. **(E)** Plots of average grayscale intensity for A1 (black), AuD (blue), AuV (red). Gray rectangles denote boundaries of L4 and L6, where the main signal peaks were centered. Scale, 250 μm.

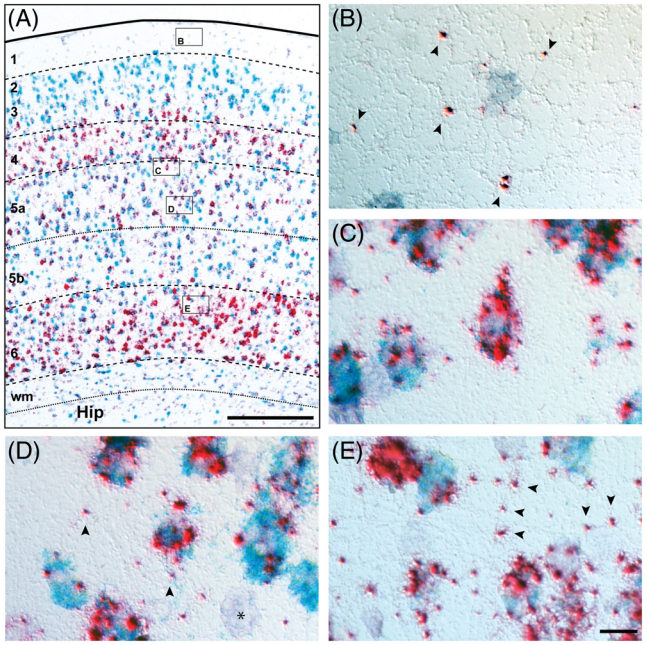

Fig. 3. Duplex chromogenic ISH in A1. *Adora1* (red) + *Gapdh* (aqua). Hematoxylin counterstain (pale blue). **(A)** *Adora1*/*Gapdh* expression across layers of A1. Insets correspond to locations of images in panels B–E. Scale bar, 250 μm. **(B–E)** 100× DIC images of inset locations in panel A. *Adora1*$^+$ puncta (red dots) are concentrated within the somatic cytoplasm, mainly in *Gapdh*$^+$ cells. Some cells, often glia (asterisk, panel D) contained no puncta. *Adora1*$^+$ puncta were also located along fine peripheral processes (arrowheads). Scale bar, 20 μm.

level. *Adora1*$^+$ puncta were concentrated within the somata of neurons and glia in A1 and MG (Figs. 3 and 4). As shown in the high-magnification images (panels B–E), puncta numbers varied between cells. Some had low numbers (<5), while high-density expression in many other cells merged and could not be individually resolved. Cells with high levels of *Gapdh* (mostly neurons) had higher concentrations of *Adora1* than cells with low *Gapdh* levels (mostly glia).

Adora1$^+$ puncta were also sparsely distributed in the neuropil, outside of somatic boundaries in A1 and MG (Figs. 3 and 4, arrowheads). DIC microscopy in panels B–E localized these along thin peripheral processes in the dense neuropil matrix, but the cells of origin could not usually be determined. The numbers of puncta not visibly localized to a cellular compartment (i.e., noise) appeared negligible. Assay specificity for *Adora1* was very high, as evidenced by the near total absence of puncta in cell-poor zones (Figs. 3B and 4B,C). Transcript expression in peripheral processes was also observed for *Aqp4* and *MBP*, described below. See Discussion for more on this subject.

3.2 Co-Expression of *Adora1* with Neuronal and Glial Markers

Multiplex fluorescence ISH (FISH) was used to demonstrate co-expression of markers within cells, and as a positive control to test probe specificity. Figure 5 shows the co-expression for neuronal and glial markers in auditory cortex (L3). In Figure 5A, *Adora1* (red) was combined

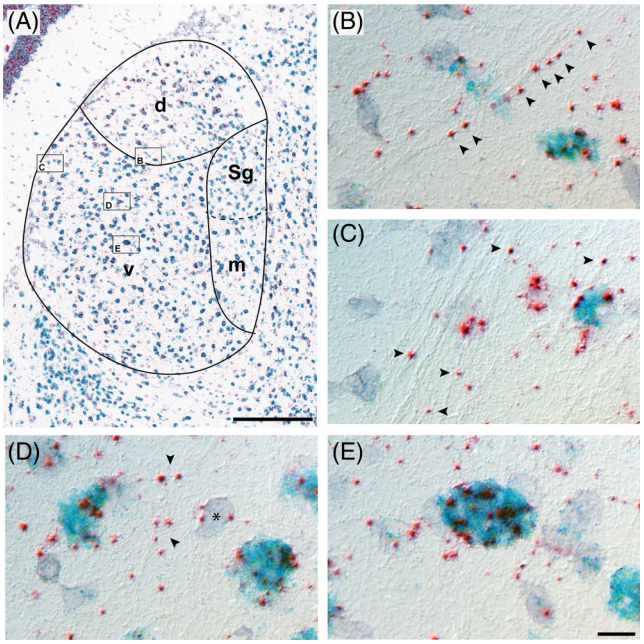

Fig. 4. Duplex chromogenic ISH in MG. *Adora1* (red) + *Gapdh* (aqua). Hematoxylin counterstain (pale blue). (**A**) *Adora1*/*Gapdh* expression across MG subdivisions (v, ventral; d, dorsal; m, medial/magnocellular) and supragenicular nucleus (Sg). Insets correspond to panels B–E. Scale bar, 250 μm. (**B–E**) 100× DIC images of inset locations in panel A. *Adora1*$^+$ puncta (red dots) are concentrated within the somatic cytoplasm, mainly in *Gapdh*$^+$ cells. Some cells, often glia (asterisk, panel D) contained few or no puncta. *Adora1*$^+$ puncta were also located along fine peripheral processes (arrowheads). Scale bar, 20 μm.

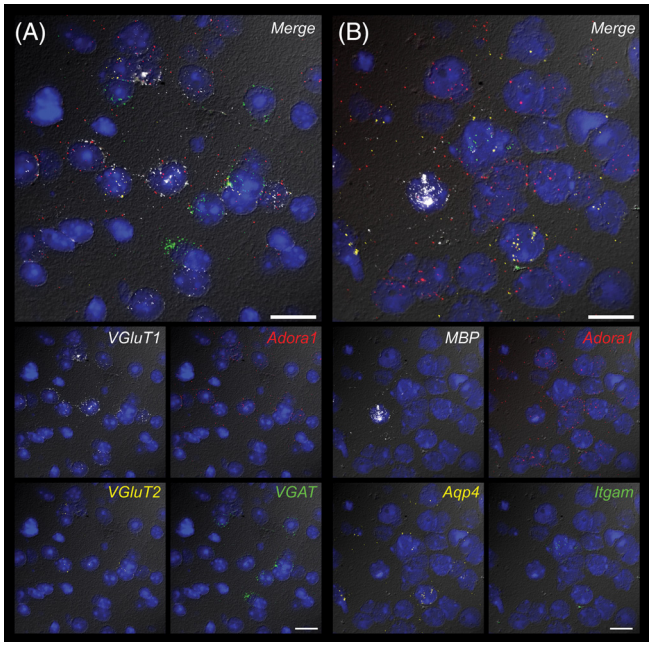

Fig. 5. Fluorescence FISH in layer 3 of A1, combining *Adora1* with neuronal or glial markers. (**A**) *Adora1* (red) with neuronal markers: *VGluT1* (white), *VGluT2* (yellow), and *VGAT* (green). (**B**) *Adora1* (red) with glial markers: *MBP*/oligodendrocytes (white), *Aqp4*/astrocytes (yellow), and *Itgam*/microglia (green). Reactive puncta (dots) of different markers do not colocalize, but may be co-expressed within the same cell (e.g., *Adora1* + *VGluT1*). Scale bar, 20 μm.

with markers for *VGluT1* (white), *VGluT2* (yellow), and *VGAT* (green). In these neurons, typical of A1 and MG, *Adora1* was co-expressed with *VGluT1* and *VGluT2*, but not *VGAT*. In Figure 5B, *Adora1* (red) was combined with markers for *MBP* (white), *Aqp4* (yellow) and *Itgam* (green). The results indicate very low (nominal) expression of *Adora1* within glia, consistent with findings in colorimetric ISH assays (see below). In all panels, the absence of co-localized signals within puncta ("dots") demonstrates that the markers of each gene were specific to their targets.

3.3 *Adora1* Expression by Neurons and Glia

In the remaining assays described below, neuronal and glial markers were paired with *Adora1* in duplex chromogenic assays. Data summaries for each combination are illustrated in Figures 6–11 (neurons) and Figures 12–17 (glia). Cell counts for all combinations are compiled in Figure 18.

Note in figures illustrating duplex labeling, DIC microscopy sometimes caused a slight z-plane distortion in the green color spectrum, affecting the appearance (size or color) of fast-green-labeled puncta. Depending on precise z-location, labeled puncta could range in color from yellow-green to blue, and could be quite small. Arrowheads were used to mark illustrative examples of small or out-of-focus puncta in some panels, where copy number was low for a given marker.

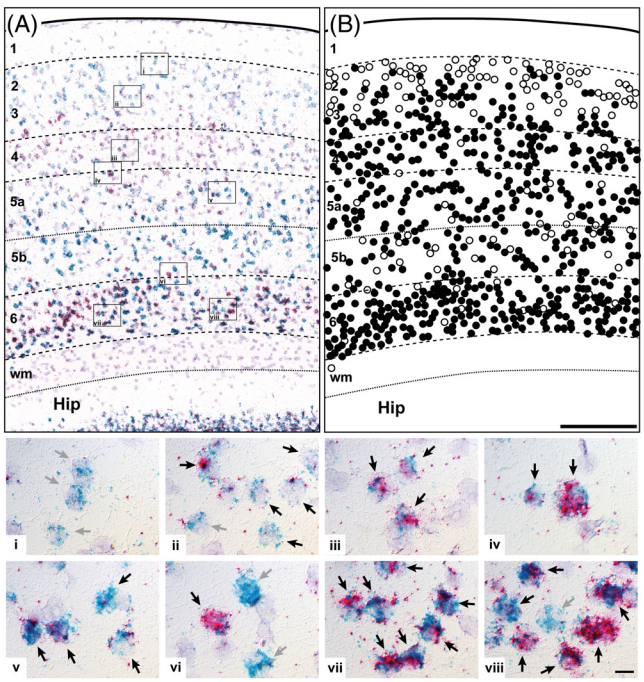

Fig. 6. Duplex chromogenic ISH in A1. *Adora1* (red) + *VGluT1* (aqua). Hematoxylin counterstain (light blue). (**A**) Bright-field image of A1. Insets correspond to panels i–viii. (**B**) *VGluT1*$^+$ cells plotted by cortical layer. Filled circles, co-expression of *Adora1* + *VGluT1*. Open circles, *VGluT1*$^+$ only. Scale bar, 250 μm. (**Panels i–viii**) 100× DIC images of inset locations in panel A. Solid arrows, dual-labeled; gray arrows, nominal *Adora1* puncta. See text for details. Scale bar, 20 μm.

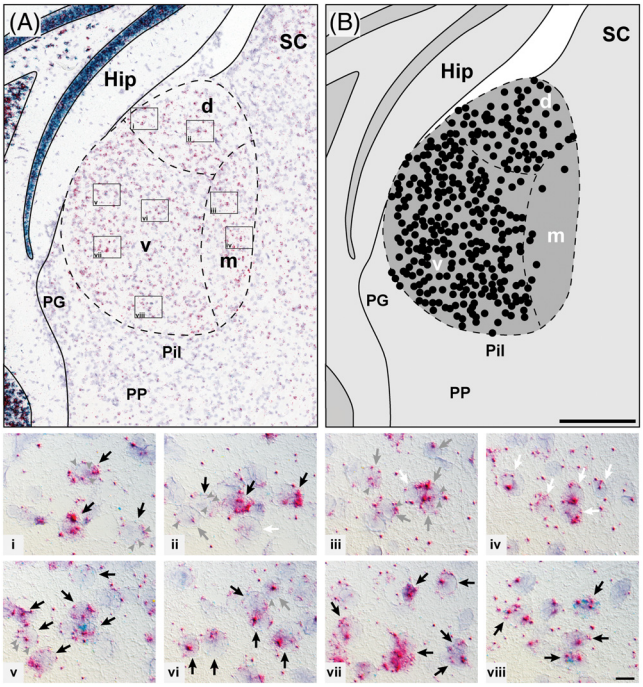

Fig. 7. Duplex chromogenic ISH in MG. *Adora1* (red) + *VGluT1* (aqua). Hematoxylin counterstain (light blue). (**A**) Bright-field image of MG. Insets correspond to panels i–viii. (**B**) *VGluT1*$^+$ cells plotted by MG subdivision. Filled circles, co-expression of *Adora1* + *VGluT1*. Open circles, *VGluT1*$^+$ only. Scale bar, 250 μm. (**Panels i–viii**) 100× DIC images of inset locations in panel A. Solid arrows, dual-labeled cells; gray arrows, nominal *VGluT1* puncta in *Adora1*$^+$ cell; white arrows, no *VGluT1* detected. Gray arrowheads in panels i–v mark examples of small and out-of-focus *VGluT1*$^+$ puncta. See text for details. Scale bar, 20 μm.

3.4 *Adora1* Expression by *VGluT1*$^+$ Neurons in A1 and MG

As previously established (Ito and Oliver, 2010; Hackett et al., 2011b; Hackett et al., 2016), *VGluT1* (*Slc17a7*) was expressed by likely all glutamatergic neurons in A1, and a majority of neurons in MGv and MGd (Figs. 6 and 7). In A1 *Adora1* was coexpressed by the majority of *VGluT1*$^+$ neurons in L3–6 (Figs. 6ii–viii and 18). Most neurons in L2 had nominal *Adora1* expression, as did a minor subpopulation of *VGluT1*$^+$ cells in other layers (Figs. 6i,vi and 18). *Adora1* transcripts were most heavily concentrated in *VGluT1*$^+$ neurons of L3b/4 and L6 (Fig. 6iii,iv,vii,viii). Strongly-labeled cells were present in other layers, as well (Fig. 6iii), indicating cell-specific variations in *Adora1* expression, independent of cortical layer.

In MG, *VGluT1* expression was largely restricted to MGv and MGd, as relatively few neurons were *VGluT1*$^+$ in MGm (Fig. 7). *VGluT1* transcript abundance was generally lower in MG neurons, compared to *VGluT2*$^+$ neurons in MG (below) or *VGluT1*$^+$ neurons in A1 (see examples in Fig. 7i,ii,v–vii). These distributions are consistent with previous findings (Barroso-Chinea et al., 2007; Ito et al., 2011; Storace et al., 2012). *Adora1* was expressed in nearly all *VGluT1*$^+$ cells in MGv and MGd, while in MGm, the majority of cells expressed *Adora1*, but not *VGluT1* (Figs. 7iii,iv and 18).

3.5 *Adora1* Expression by *VGluT2*$^+$ Neurons in A1 and MG

In A1, *VGluT2* (*Slc17a6*) was expressed by a minor subpopulation of neurons that co-express *VGluT1*, mainly in L3/4, as previously reported (Ito and Oliver, 2010, Hackett et al., 2011b, Hackett et al., 2016). *VGluT2* transcript abundance was relatively low in most cells, compared with *VGluT1* (Fig. 8i–viii). All of the *VGluT2*$^+$ neurons identified in A1 coexpressed *Adora1*, regardless of layer (Figs. 8 and 18).

In MG, *VGluT2* expression was strong in nearly all neurons in all divisions (Figs. 9 and 18). The vast majority co-expressed *Adora1*. *VGluT2*$^+$ cells with nominal *Adora1* expression were rare in MGv and MGd, while slightly more were found in MGm/Sg (Figs. 9iii and 18).

3.6 *Adora1* Expression by *VGAT*$^+$ Neurons in A1 and MG

In A1, *VGAT* (*Slc32a1*) was expressed by GABAergic neurons in all layers, with occasional labeling of cells in the white matter (Figs. 10 and 18). *Adora1* expression by the majority of *VGAT*$^+$ neurons was absent or nominal (Fig. 10i,ii,v,vi–viii), and low-abundance co-expression was observed in a minority of GABAergic neurons scattered across L3–L6 (Fig. 10ii,iv). While the somata of many *VGAT*$^+$ cells were isolated from other cell types by neuropil, others were closely opposed to one or more unlabeled cells (likely glia) (Fig. 10i–iv,vii). At the border between these cells, the clustering of *Adora1* transcripts

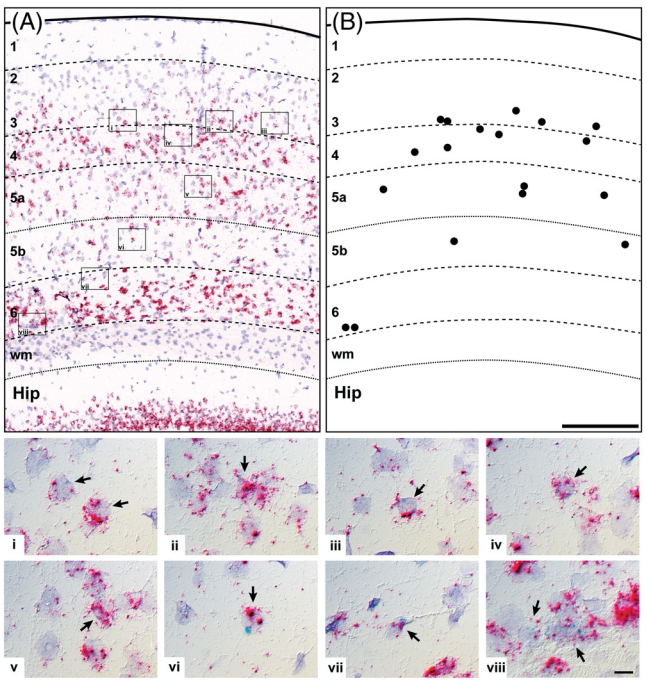

Fig. 8. Duplex chromogenic ISH in A1. *Adora1* (red) + *VGluT2* (aqua). Hematoxylin counterstain (light blue). (**A**) Bright-field image of A1. Insets correspond to panels i–viii. (**B**) *VGluT2*$^+$ cells plotted by cortical layer. Filled circles, co-expression of *Adora1* + *VGluT2*. Scale bar, 250 μm. (**Panels i–viii**) 100× DIC images of inset locations in panel A. Solid arrows, dual-labeled. Note low *VGluT2* expression levels. See text for details. Scale bar, 20 μm.

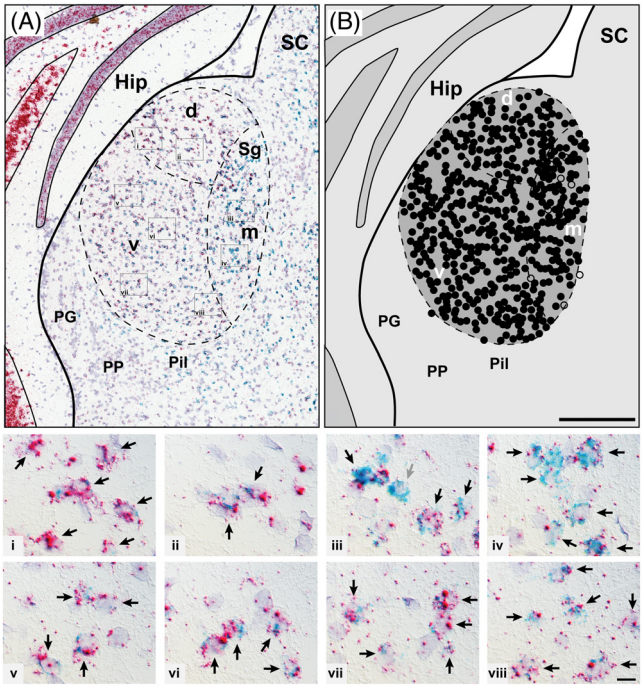

Fig. 9. Duplex chromogenic ISH in MG. *Adora1* (red) + *VGluT2* (aqua). Hematoxylin counterstain (light blue). (**A**) Bright-field image of MG. Insets correspond to panels i–viii. (**B**) *VGluT2*$^+$ cells plotted by MG subdivision. Filled circles, co-expression of *Adora1* + *VGluT2*. Open circles, *VGluT2*$^+$ only. Scale bar, 250 μm. (**Panels i–viii**) 100× DIC images of inset locations in panel A. Solid arrows, dual-labeled; gray arrows, nominal *Adora1* puncta. See text for details. Scale bar, 20 μm.

was common. For plotting, inspection at 100×, DIC was usually required to determine whether the transcripts were located within the *VGAT*$^+$ cell or the apposed cell. Most often it was the latter.

In the MG of rodents, GABAergic cells (and therefore *VGAT*$^+$ neurons) are uncommon (Winer and Larue, 1996; Ito et al., 2011; Yuge et al., 2011; Hackett et al., 2016). Consistent with this prior research, the MG contained very few *VGAT*$^+$ cells (Figs. 11 and 18) (note the reduced *y*-axis scale in Fig. 18). There was a slight tendency for *VGAT*$^+$ cells to more often be found in MGm/Sg. Overall, *Adora1* was expressed at low levels by roughly half of the sparse population of *VGAT*$^+$ cells identified anywhere within the MG, with comparable low expression in adjacent nuclei, where *VGAT*$^+$ cells were abundant.

3.7 *Adora1* Expression by *MBP*$^+$ Cells in A1 and MG

In A1, *MBP* was expressed in the somata of myelinating oligodendrocytes in L2–L6, and in very high numbers in the underlying white matter (Figs. 12 and 18). *Adora1* was coexpressed by roughly half of the *MBP*$^+$ cells in L2–L5 and 66% in L6. In the white matter, only 34% of *MBP*$^+$ cells coexpressed *Adora1* (Figs. 12viii and 18). Overall, *Adora1* transcript abundance in the cytoplasm of *MBP*$^+$ somata was modest, as evident in Figure 12i–viii (black arrows). *Adora1*$^+$ puncta were typically localized near the cell membrane and at the base of peripheral processes extending away from the soma (Fig. 12iv,vi, gray arrowheads).

In addition to dense concentrations in the somatic cytoplasm, *MBP*$^+$ puncta were also located in peripheral processes, distant from cell somata, visible in all panels in Figure 12. The DIC images (Fig. 12i–viii, arrowheads) reveal that puncta were typically located in thin processes, often distributed along the trajectory of a single process (Fig. 12iii,v, black arrowheads). Such processes were found in L1–L6, and especially dense in white matter tracts (Fig. 12vii,viii, arrowheads). As discussed above, extrasomatic *Adora1*$^+$ transcripts could be located along peripheral processes. Typically, extrasomatic *MBP*$^+$ and *Adora1*$^+$ puncta were not contiguous within processes, but closely apposed puncta were sometimes observed (Fig. 12ii), suggesting that local translation of both proteins may sometimes occur in contiguous subcellular compartments.

In MG, *MBP*$^+$ cells were evenly distributed across divisions (Fig. 13A). Transcript abundance in the somatic cytoplasm was typically high (Fig. 13i–viii). As in cortex, *MBP*$^+$ puncta were also abundant within extrasomatic processes, often forming continuous trajectories that could be followed for 300 μm, or more, visible as long striations in Figure 13A,v,vii. These were especially conspicuous in MGv. *Adora1* expression was nominal in the majority of *MBP*$^+$ cells in all divisions (Figs. 13B and 18). These tended to be located at or near the somatic periphery, often at the base of peripheral processes (Fig. 13I,iii, iv,vi–viii). In the neuropil, *Adora1*$^+$ puncta were

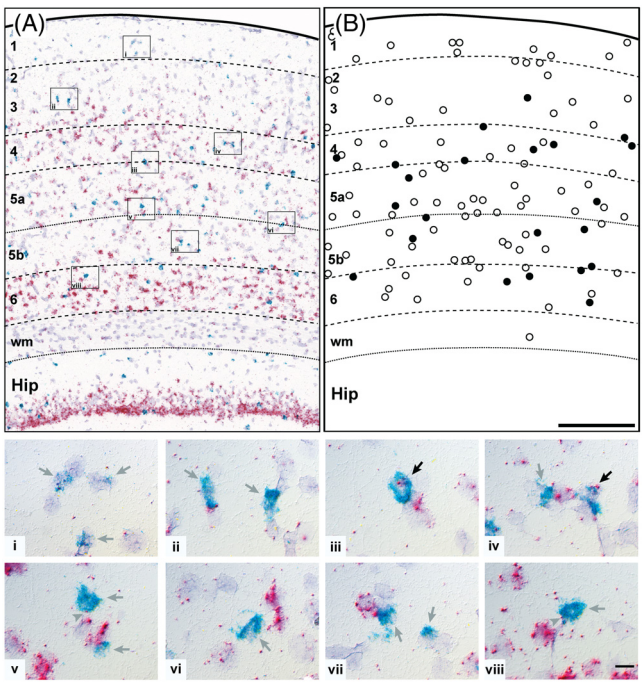

Fig. 10. Duplex chromogenic ISH in A1. *Adora1* (red) + *VGAT* (aqua). Hematoxylin counterstain (light blue). (**A**) Bright-field image of A1. Insets correspond to panels –i–viii. (**B**) *VGAT*$^+$ cells plotted by cortical layer. Filled circles, co-expression of *Adora1* + *VGAT*. Open circles, *VGAT* only. Scale bar, 250 μm. (**Panels i–viii**) 100× DIC images of inset locations in panel A. Solid arrows, dual-labeled; gray arrows, nominal *Adora1* puncta. See text for details. Scale bar, 20 μm.

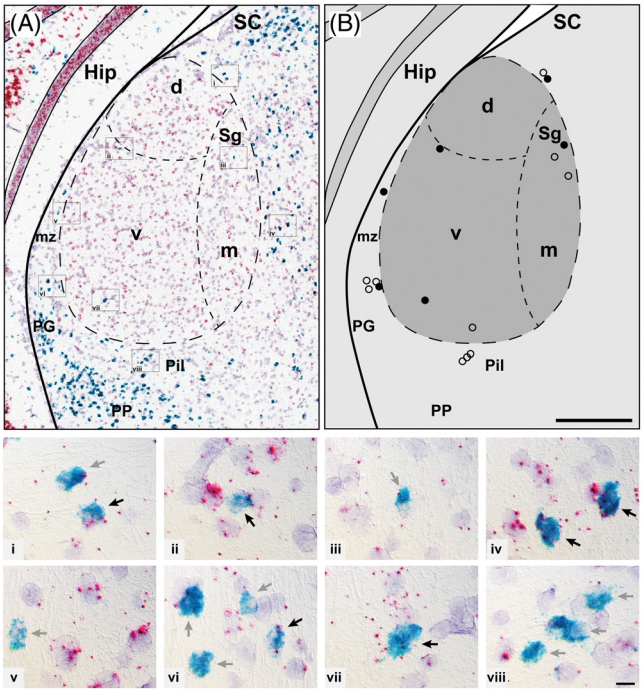

Fig. 11. Duplex chromogenic ISH in MG. *Adora1* (red) + *VGAT* (aqua). Hematoxylin counterstain (light blue). (**A**) Bright-field image of MG. Insets correspond to panels –i–viii. (**B**) *VGAT*$^+$ cells plotted by MG subdivision. Filled circles, co-expression of *Adora1* + *VGAT*. Open circles, *VGAT*$^+$ only. Scale bar, 250 μm. (**Panels i–viii**) 100× DIC images of inset locations in panel A. Solid arrows, dual-labeled; gray arrows, nominal *Adora1* puncta. See text for details. Scale bar, 20 μm.

occasionally located among *MBP*$^+$ puncta within the same peripheral processes.

3.8 *Adora1* Expression by *Aqp4*$^+$ Cells in A1 and MG

In A1, *Aqp4* was expressed by astrocytes within all cortical layers, white matter, pial membranes, and adjacent to blood vessels (Figs. 14 and 18). *Adora1* was co-expressed in subpopulations of *Aqp4*$^+$ cells in L2–L6 and white matter. The highest concentration of co-labeled cells was in L6 (Fig. 14B). As for the other glial cells, *Adora1* transcript abundance was low in astrocytes, compared to neurons (Fig. 14i–viii). The perivascular (Fig. 14ii) and pial astrocytes (Fig. 14i) typically had little to no detectable expression of *Adora1*. *Aqp4*$^+$ puncta were contained within the somatic cytoplasm of most cells, but some were located along fine processes in the extracellular neuropil in all cortical layers.

In MG, *Aqp4*$^+$ cells were distributed evenly across divisions (Figs. 15 and 18). *Adora1* was expressed by most of the astrocytes detected by *Aqp4*. As in A1, *Adora1* transcript abundance was typically low in *Aqp4*$^+$ cells within the main body of the MG, and nominal in most perivascular and pial astrocytes (Fig. 15i–viii). This distinction signals a potential difference in adenosine signaling between astrocytes in these domains in both A1 and MG. *Aqp4*$^+$ puncta were also common in fine peripheral processes in the neuropil, and outside of somata along pial and vascular membranes.

3.9 *Adora1* Expression by *Itgam*$^+$ Cells in A1 and MG

In A1, *Itgam*$^+$ cells were relatively evenly distributed across cortical layers, with higher numbers in white matter (Figs. 16 and 18). Microglia were often spatially isolated from other cells (Fig. 16v), but many were found closely opposed to neurons or other cells (Fig. 16i–iv), consistent with recent studies (Baalman et al., 2015). The majority of *Itgam*$^+$ cells did not co-express *Adora1*, but often contained 1 or 2 *Adora1*$^+$ puncta (gray arrowheads in Fig. 16i–viii). *Itgam*$^+$ puncta were largely confined to somatic cytoplasm, and rarely found in the neuropil along processes.

In MG, *Itgam*$^+$ cells were sparsely distributed across divisions, compared to astrocytes and oligodendrocytes (Figs. 17 and 18). As in cortex, the majority did not co-express *Adora1*, and *Adora1* transcript abundance in cells identified as co-labeled was generally very low (near the cutoff of 3 *Adora1*$^+$ puncta).

3.10 A_1R Immunohistochemistry (IHC, FIHC)

Chromogenic (IHC) and fluorescence (FIHC) assays revealed strong punctate A_1R immunoreactivity in A1 and MG. Reactivity was concentrated in the neuropil, characterized by dense perisomatic labeling (Fig. 19A,B)

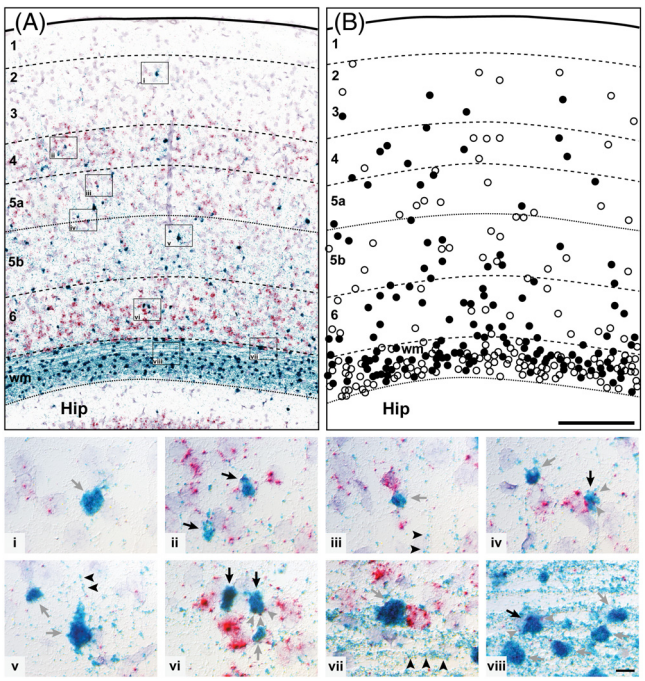

Fig. 12. Duplex chromogenic ISH in A1. *Adora1* (red) + *MBP* (aqua). Hematoxylin counterstain (light blue). (**A**) Bright-field image of A1. Insets correspond to panels –i–viii. (**B**) *MBP*$^+$ cells plotted by cortical layer. Filled circles, co-expression of *Adora1* + *MBP*. Open circles, *MBP* only. White matter, wm. Scale bar, 250 μm. (**Panels i–viii**) 100× DIC images of inset locations in panel A. Solid arrows, dual-labeled; gray arrows, nominal *Adora1* puncta. Arrowheads, extrasomatic *MBP*$^+$ puncta (black) and *Adora1*$^+$ puncta (gray). See text for details. Scale bar, 20 μm.

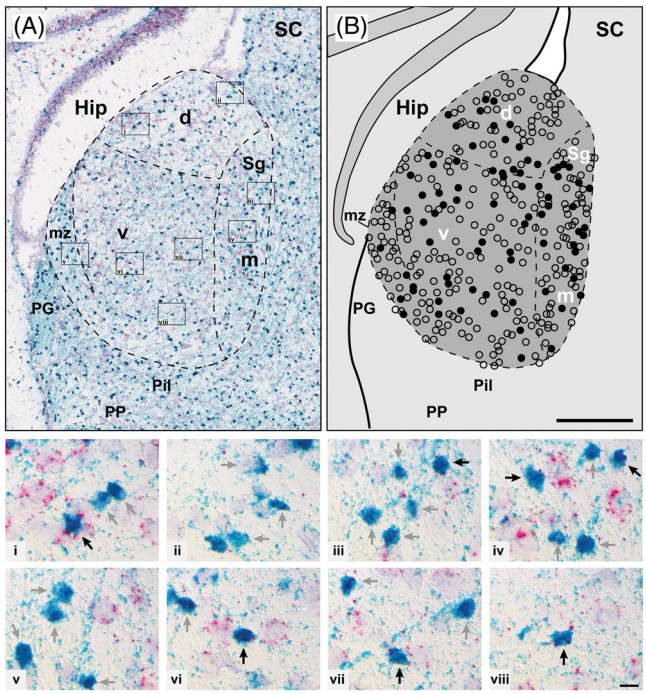

Fig. 13. Duplex chromogenic ISH in MG. *Adora1* (red) + *MBP* (aqua). Hematoxylin counterstain (light blue). (**A**) Bright-field image of MG. Insets correspond to panels –i–viii. (**B**) MBP^+ cells plotted by MG subdivision. Filled circles, co-expression of *Adora1* + *MBP*. Open circles, MBP^+ only. Scale bar, 250 μm. (**Panels i–viii**) 100× DIC images of inset locations in panel A. Solid arrows, dual-labeled; gray arrows, nominal *Adora1* puncta. See text for details. Scale bar, 20 μm.

around most cells (Fig. 19A,B). Sparse labeling was also observed in the somatic cytoplasm, mainly in neurons ($DAPI^+/NeuN^+$), but not presumptive glia ($DAPI^+/NeuN^-$) (Fig. 19D–F). In A1, immunoreactivity was strong across L2–L6, but the density of reactive puncta was relatively high in L4 (Fig. 19A), compared to other layers (e.g., L6) (Fig. 19B) (qualitative impression). In addition to dense perisomatic and neuropil labeling, immunoreactive puncta sometimes formed orderly distributions (strings) along peripheral processes. Examples are shown in Figure 19D,E. These striations were evident in the densely reactive neuropil of L3/L4 (Fig. 19D), and also in L5/L6, where puncta were sometimes localized along apical dendrites (Fig. 19E, arrowheads). These patterns are similar to an earlier study in other forebrain areas using a custom antibody (Ochiishi et al., 1999), in which A_1Rs were localized to pre- and postsynaptic compartments of neurons.

4. DISCUSSION

The main purpose of this study was to map the distributions of neuronal and glial cell types that express *Adora1* transcripts in the auditory forebrain of adult mice. A general finding was that *Adora1* is strongly expressed by the vast majority of glutamatergic neurons in A1 and MG, and expressed at lower levels by subpopulations of GABAergic neurons, astrocytes, myelinating oligodendrocytes, and microglia. These patterns reveal regional and cell-type specificity in *Adora1* expression, and suggest functional differences in adenosine signaling mediated by the A_1R receptor.

The discussion begins with a brief overview of adenosine signaling, which depends heavily on studies in hippocampus, striatum, and other brain regions. This is followed by discussion of A_1R-mediated contributions to synaptic plasticity in the auditory forebrain. The balance of the discussion is devoted to integrating the findings of this study with existing models of auditory forebrain circuitry, along with directions for future study.

4.1 Sources of Adenosine and A_1R-Mediated Signaling in the Forebrain

Adenosine plays important roles in the modulation of neuronal activity and neuro–glial interactions in the brain (Burnstock, 2007; Boison, 2008a; Abbracchio et al., 2009; Housley et al., 2009; Koles et al., 2016). Multiple sources of extracellular adenosine have been identified, and their respective contributions in this complex system continue to be studied. The two main categories are direct release by neurons and an indirect process involving catabolism of ATP released by neurons and glia (Fig. 20C) (Fredholm et al., 2005; Wall and Dale, 2013; Sebastiao and Ribeiro, 2015; Cunha, 2016). Direct neuronal release of adenosine, which may be pre- or postsynaptic, appears to be the main source and is achieved by vesicle-mediated excocytosis or translocation through bidirectional equilibrative nucleoside transporters (ENTs)

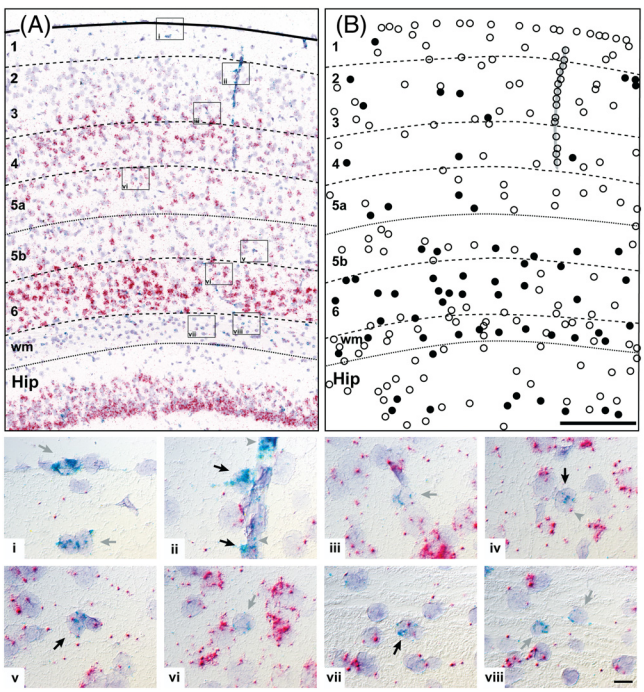

Fig. 14. Duplex chromogenic ISH in A1. *Adora1* (red) + *Aqp4* (aqua). Hematoxylin counterstain (light blue). (**A**) Bright-field image of A1. Insets correspond to panels –i–viii. (**B**) $Aqp4^+$ cells plotted by cortical layer. Filled circles, co-expression of *Adora1* + *Aqp4*. Open circles, *Aqp4* only. White matter, wm. Scale bar, 250 μm. (**Panels i–viii**) 100× DIC images of inset locations in panel A. Solid arrows, dual-labeled; gray arrows, nominal *Adora1* puncta. Arrowheads, perivascular $Aqp4^+$ puncta (gray). See text for details. Scale bar, 20 μm.

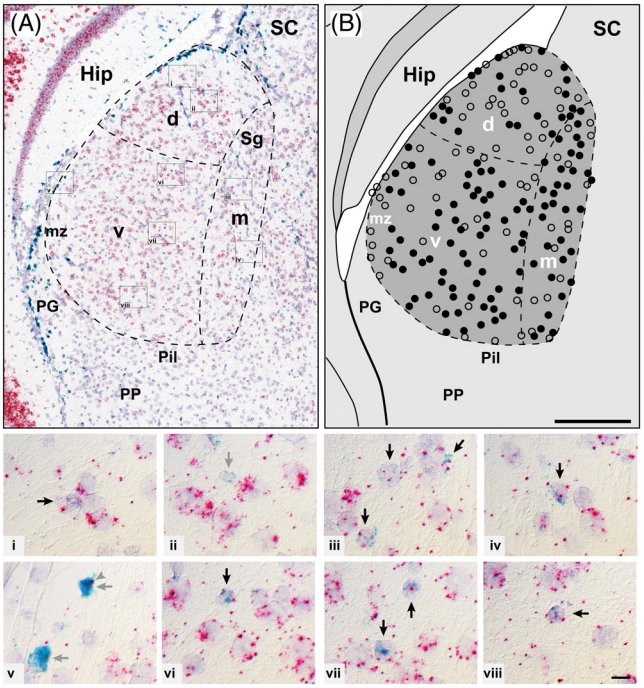

Fig. 15. Duplex chromogenic ISH in MG. *Adora1* (red) + *Aqp4* (aqua). Hematoxylin counterstain (light blue). (**A**) Bright-field image of MG. Insets correspond to panels –i–viii. (**B**) *Aqp4*$^+$ cells plotted by MG subdivision. Filled circles, co-expression of *Adora1* + *Aqp4*. Open circles, *Aqp4*$^+$ only. Scale bar, 250 μm. (**Panels i–viii**) 100× DIC images of inset locations in panel A. Solid arrows, dual-labeled; gray arrows, nominal *Adora1* puncta. Arrowhead (panel v), single *Adora1* puncta within an *Aqp4*$^+$ cell. See text for details. Scale bar, 20 μm.

(Fredholm and Hedqvist, 1980; Mitchell et al., 1993; Manzoni et al., 1994; Brundege and Dunwiddie, 1996; Wall and Dale, 2008; Klyuch et al., 2012; Lovatt et al., 2012; Melani et al., 2012). ATP released by glia and neurons may be converted to AMP and adenosine by ectonucleotidases (ENase), including ecto-5′-nucleotidase (Nt5e) (Lloyd et al., 1993; Zhang et al., 2003; Pascual et al., 2005; Lovatt et al., 2012; Zimmermann et al., 2012; Lalo et al., 2014). Basal levels of extracellular adenosine are typically maintained at low concentrations (Cunha, 2001; Boison, 2006), sufficient to affect tonic activation of A_1Rs and inhibitory tone (Fredholm, 2007, 2012; Lalo et al., 2014). ENTs on neurons and glia (especially astrocytes) at the synapse help to maintain basal levels and restore balance after activity-related increases in extracellular adenosine levels, which primarily result from neuronal release (Fredholm et al., 2005; Dale, 2008; Boison et al., 2010; Lovatt et al., 2012). ENT activity is regulated by adenosine receptor activation through intracellular protein kinase pathways (e.g., adenosine kinase, ADK) responsible for adenosine metabolism (Boison, 2013).

Adenosine signaling is mainly achieved through G-protein-coupled A_1Rs, the most highly expressed of the four receptor subtypes. In neurons, A_1Rs occupy pre- and postsynaptic sites, but abundance appears to be highest in presynaptic terminals (Tetzlaff et al., 1987; Ochiishi et al., 1999; Rebola et al., 2003; Rebola et al., 2005). The primary action of A_1R-mediated adenosine signaling at excitatory synapses is presynaptic inhibition of glutamate release, which is increased by interfering with A_1R activation (Fredholm and Dunwiddie, 1988; Dunwiddie and Masino, 2001; Fredholm et al., 2005). Postsynaptic effects involving A_1Rs include decreased activation of ionotropic NMDA receptors and ion channel conductances (Proctor and Dunwiddie, 1987; Klishin et al., 1995a; Klishin et al., 1995b; Wetherington and Lambert, 2002; Chung et al., 2009; Kim and Johnston, 2015). Through these mechanisms, activity-dependent adenosine signaling through A_1Rs contributes to adaptive changes in neurotransmission associated with various processes, such as neuroprotection and plasticity.

4.2 Adenosine Signaling and Synaptic Plasticity in the Auditory Forebrain

The mechanisms that contribute to synaptic plasticity in the auditory forebrain remain the subject of intensive research, as their elucidation is essential for improved understanding of learning and memory (Weinberger, 2007), reorganization/augmentation of stimulus representations (Fritz et al., 2007; Sanes and Bao, 2009; Schreiner and Polley, 2014), and critical periods (Bavelier et al., 2010; Froemke and Jones, 2011; Takesian and Hensch, 2013). Critical periods form as synaptic machinery stabilizes during postnatal development, and plasticity at both corticocortical and thalamocortical synapses is dampened, limiting the changes in activity that can be induced by

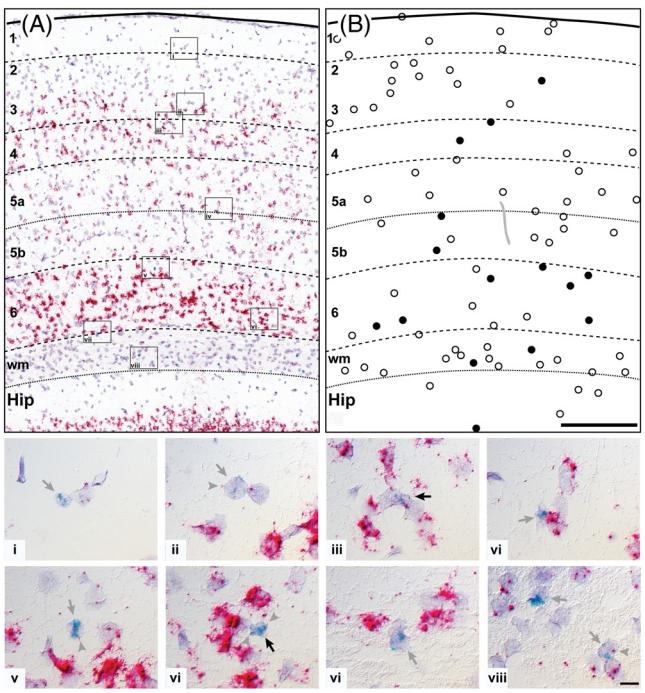

Fig. 16. Duplex chromogenic ISH in A1. *Adora1* (red) + *Itgam* (aqua). Hematoxylin counterstain (light blue). (**A**) Bright-field image of A1. Insets correspond to panels –i–viii. (**B**) *Itgam*$^+$ cells plotted by cortical layer. Filled circles, co-expression of *Adora1* + *Itgam*. Open circles, *Itgam* only. White matter, wm. Scale bar, 250 μm. (**Panels i–viii**) 100× DIC images of inset locations in panel A. Solid arrows, dual-labeled; gray arrows, nominal *Adora1* puncta. Arrowhead (panels v, viii), single *Adora1*$^+$ puncta within an *Adora1*$^+$ cell. See text for details. Scale bar, 20 μm.

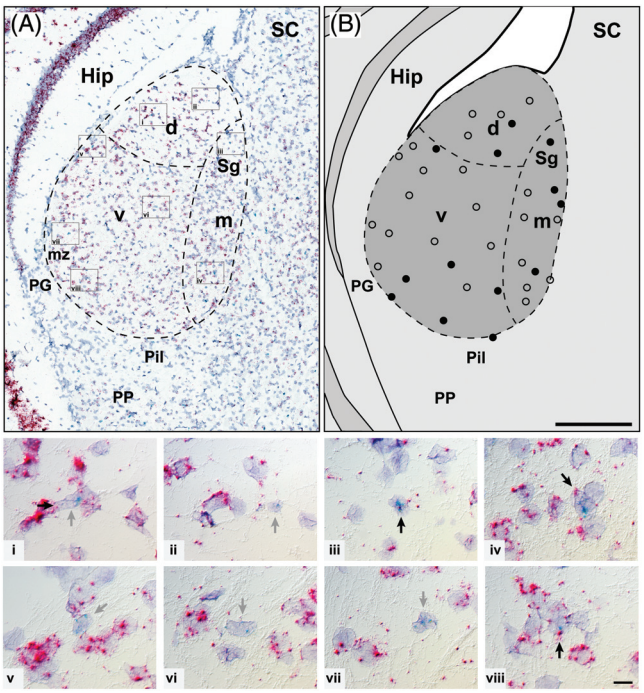

Fig. 17. Duplex chromogenic ISH in MG. *Adora1* (red) + *Itgam* (aqua). Hematoxylin counterstain (light blue). (**A**) Bright-field image of MG. Insets correspond to panels –i–viii. (**B**) *Itgam*$^+$ cells plotted by MG subdivision. Filled circles, co-expression of *Adora1* + *Itgam.* Open circles, *Itgam*$^+$ only. Scale bar, 250 μm. (**Panels i–viii**) 100× DIC images of inset locations in panel A. Solid arrows, dual-labeled; gray arrows, nominal *Adora1* puncta. See text for details. Scale bar, 20 μm.

experience (Zhang and Poo, 2001; Sanes and Woolley, 2011). Thalamocortical synapses become especially resistant to change with maturation (Crair and Malenka, 1995; Barkat et al., 2011; Chun et al., 2013), whereas prior to critical period closure, even passive exposure to a sound is sufficient to induce changes (Zhang et al., 2001; de Villers-Sidani et al., 2007; Insanally et al., 2009; Barkat et al., 2011). Yet, plasticity can still be induced in mature TC and CC synapses by an active process, such as attention to behaviorally relevant sounds (Recanzone et al., 1993; Blake et al., 2002; Edeline, 2003; Keeling et al., 2008; Sarro et al., 2015), electrical stimulation of MG (Jafari et al., 2007; Ma and Suga, 2009; Zhu et al., 2014), or other forms of neuromodulation (Edeline, 2003; Metherate, 2004; Metherate and Hsieh, 2004; Weinberger, 2004; Froemke and Jones, 2011; Metherate, 2011; Edeline, 2012; Blundon and Zakharenko, 2013; Takesian and Hensch, 2013). For example, merely pairing the release of acetylcholine with a sound is sufficient to increase neuronal responsiveness to that stimulus (Bao et al., 2003).

Taken together, these findings imply that plasticity becomes limited during maturation by the establishment of gating mechanisms, which can subsequently be altered under various conditions to permit plasticity. Although many factors are very well known (e.g., acetylcholine, GABA), the roles of other players, such as adenosine, continue to be identified and refined. In hippocampus and other brain regions, adenosine can regulate synaptic transmission and plasticity through A_1 and A_{2a} receptors, located at pre- and postsynaptic sites on neurons and astrocytes (Sebastiao and Ribeiro, 2009; Sperlagh and Vizi, 2011; Dias et al., 2013; Ota et al., 2013; Chen et al., 2014; Sebastiao and Ribeiro, 2015). In somatosensory cortex, for example, adenosine application downregulated glutamate release from TC synapses, while A_1R inhibition prevented this effect, enabling the modulation of short-term plasticity (Ferrati et al., 2016).

In auditory cortex, a series of studies revealed that adenosine signaling through A_1Rs is a major factor in gating thalamocortical (TC) plasticity after the early critical period. Blundon et al. (2011) showed that postsynaptic LTD depends on group 1 metabotropic glutamate receptors ($mGluR_1$), but is gated *presynaptically* at mature synapses in A1 by mechanisms that involve adenosine. Briefly, they found that activation of presynaptic M_1 acetylcholine receptors (M_1Rs) interfered with adenosine-A_1R signaling downstream, permitting sustained glutamate release and LTD induction. Further, inhibition or deletion of A_1Rs was sufficient to release this gating. Chun et al. (2013) showed that postsynaptic LTP in TC synapses in A1 also depends on Group 1 mGluRs ($mGluR_1$, $mGluR_5$), but not NMDARs, and becomes gated during maturation. In A1 of adult animals, TC LTP could be induced by combining cholinergic release with disinhibition, but not by either mechanism alone. As in the LTD study, cholinergic activation triggered sustained glutamate release by negative regulation of adenosine-A_1R signaling, unmasking LTP. In $A_1R^{-/-}$ knockout mice, LTP could be induced even when M_1Rs were blocked, indicating that the cholinergic inputs are not required when A_1Rs have been removed. Most recently, this line of work was extended by this group to receptive field plasticity, *in vivo* (Blundon et al., 2017). As noted above, passive exposure to a pure tone in an enriched acoustic environment is sufficient to alter receptive fields and expand map representation of that tone in A1 neurons of immature animals, but not adults. In this study, interfering with A_1Rs in the MG of adult animals by any of several methods (deletion, knockdown, and inhibition) restored map plasticity in A1 and improved tone discrimination after pairing with passive exposure to a pure tone probe. A_1R agonists inhibited map plasticity. Thus, the maturation of adenosine-A_1R signaling in TC synapses acts as a gate, limiting the expression of TC plasticity in adults. Removal of that gating mechanism enables TC synaptic plasticity (Fig. 20c).

The time course of these effects parallels the maturational trajectory of adenosine receptor expression in the mouse auditory forebrain. In previous work, we generated whole genome transcriptome profiles of A1 and MG, highlighting expression trajectories for over 200 gene families at key stages during postnatal development in mice (P7, P14, P21, adult) (Hackett et al., 2015; Guo et al., 2016). For the adenosine receptor family, *Adora1* transcript expression was dominant in A1 and MG, compared to very low expression of *Adora2a* and *Adora2b* (Fig. 1), consistent with studies in other brain regions (Cahoy et al., 2008; Zhang et al., 2014; Zeisel et al., 2015). We also found that *Adora1* expression increased sharply from P7 to P14 in A1 and MG, and then remained elevated through adulthood. This upregulation is notable, as the P7–P14 interval spans the period before and after hearing onset, and the closing of the early critical period (de Villers-Sidani et al., 2007, Insanally et al., 2009,

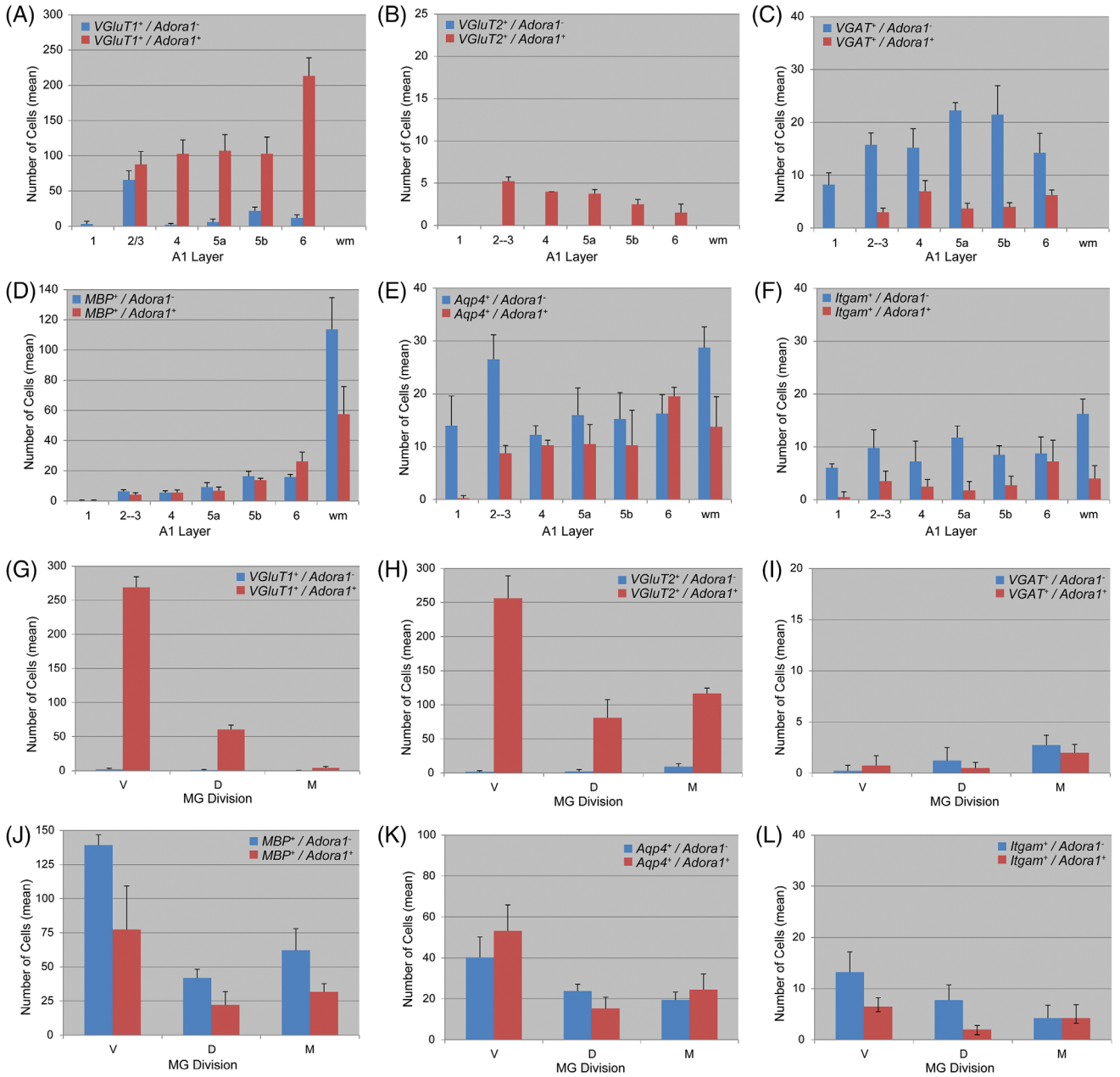

Fig. 18. Cell counts in A1 and MG for each marker combination. Histograms reflect the mean number of single- (blue bars) and dual-labeled cells (red bars) for each cell type marker. (**A–C**) Neuronal subtypes + *Adora1* in A1 by cortical layer. (**D–E**) Glial subtypes + *Adora1* in A1. (**G–I**) Neuronal subtypes + *Adora1* in MG by division. (**J–L**) Glial subtypes + *Adora1* in MG. Error bars, standard deviation. Note variations in *y*-axis scale between panels.

Barkat et al., 2011). Rapid upregulation during this period has been noted in other brain regions (Rivkees, 1995). In addition, we found that expression of several neurotransmitter receptors (e.g., M_1R) and numerous coding and noncoding genes known to be involved in critical periods plasticity were in flux during this time interval, suggesting that activity-dependent mechanisms may alter expression among networks of genes (Hackett et al., 2015; Guo et al., 2016; Hackett et al., 2016).

Although not a focus of this study, it may be important context for future purposes that several P_2 ATP receptors were significantly expressed in the auditory forebrain, and that levels changed from P7 to adult (Fig. 1). For example, *P2rx2* was expressed at low levels at P7, then dropped to nominal levels by P14; *P2rx4* expression steadily increased from P7 to adult; and *P2ry12* increased sharply from P7 to P14 in A1 and MG. The roles of P_2 receptors are poorly understood in sensory forebrain regions, but intensive studies elsewhere in the brain reveal important roles in plasticity and development (Zimmermann, 2011; Sebastiao and Ribeiro, 2015). Thus, there is likely much more to learn about purinergic and

other signaling mechanisms with respect to synaptic plasticity and the establishment of critical periods. These data can serve to guide focused inquiries.

4.3 *Adora1* Expression by Neurons in the MG

In the MG, *Adora1* expression by neurons was almost entirely restricted to glutamatergic neurons, as GABAergic neurons are rare in the rodent MG. Expression was uniform within and across subdivisions, implying that adenosine utilization is comparable across the cell populations within parallel pathways represented in the MG (Fig. 20A). These results indicate that A_1R-adenosine signaling could impact the presynaptic activity of TC projections MG to all areas of auditory cortex (primary and secondary), as well as descending projections to auditory brainstem (e.g., inferior colliculus). These patterns are consistent with autoradiographic binding studies of A_1Rs in several species (Fastbom et al., 1987), and also support recent observations (discussed above) that A_1Rs located on TC terminals in L3/L4 of A1 modulate presynaptic glutamate release with profound effects on excitatory transmission and synaptic plasticity (Blundon and Zakharenko, 2013; Chun et al., 2013; Blundon et al., 2017).

With this functionality in mind, the expression patterns in MG raise several questions for consideration and future study. First, do presynaptic A_1Rs on TC projections modulate glutamate release in other thalamorecipient layers of auditory cortex (e.g., L1, L6)? This is a reasonable hypothesis, given that MG neurons co-express *VGluT2* and *Adora1* transcripts, and immunoreactive terminals are present in all thalamorecipient layers (Fig. 19) (Hackett et al., 2011b; Hackett et al., 2016). Second, does adenosine signaling mediate the same functions in auditory cortical areas other than A1? Strong *Adora1* expression in all MG subdivisions suggests that presynaptic A_1 receptors are localized on TC inputs to all areas of auditory cortex, not just A1 (Fig. 20A). Third, do the descending projections of MG neurons to the inferior colliculus and other subcortical targets bear presynaptic A_1 receptors? If so, are they also involved in the modulation of glutamate release? This seems likely, given that A_1R-adenosine signaling has similar effects across brain regions (Cunha, 2016).

4.4 *Adora1* Expression by Neurons in A1

As summarized in Figure 20A, inputs to A1 include laminar-specific thalamic and cortical projections, mainly from MG and from other auditory cortical fields. The downstream targets of A1 projection neurons vary by layer of origin, and include both cortical and subcortical targets in both hemispheres. The findings of this study indicate that *Adora1* was expressed by the majority of glutamatergic neurons in L3–L6 of A1, based on co-expression with *VGluT1* and/or *VGluT2*. In contrast, *Adora1* was expressed with relatively low abundance in a small subpopulation of GABAergic neurons. Expression varied by layer, characterized by the highest levels in L6, intermediate in L3–L5, and nominal in L1–L2. These laminar patterns were maintained in the belt areas surrounding A1, as well as in frontal and other sensory cortical regions (data not shown), suggesting common organizational principles across cortical fields.

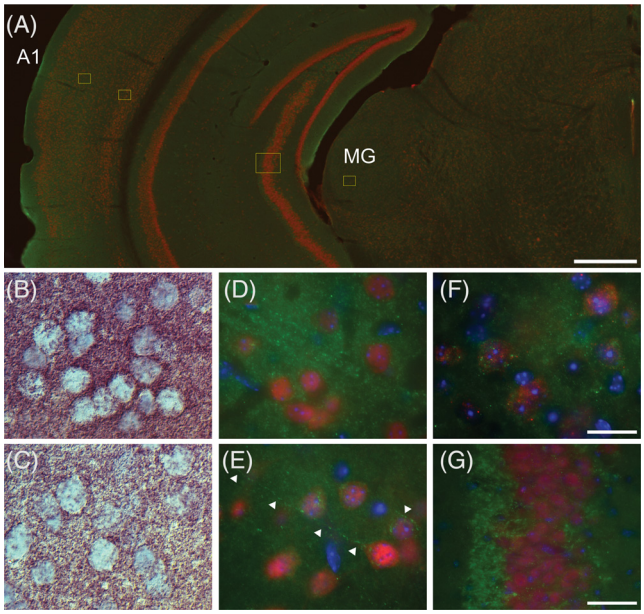

Fig. 19. *Adora1* (A_1R) IHC. (A) A_1R (green) and NeuN (red) FIHC. Low-magnification view of auditory forebrain and surrounding structures. Insets correspond to panels D–G. (**B, C**) Bright-field images of single chromogen A_1R IHC in A1 layer 4 (**B**) and layer 6 (**C**). (**D, E**) FIHC showing A_1R (green), NeuN (red), and DAPI (blue). (**D**) A1 layer 4. (**E**) A1 layer 6. Arrowheads show strings of A_1R-immunoreactive puncta. (**F**) MGv. (**G**) CA3 region of hippocampus. Scale bars: (**A**) 500 μm; (**B–F**) 20 μm; (**G**) 50 μm.

A_1R immunohistochemistry revealed dense punctate expression in the neuropil and perisomatic domains, suggesting utilization of A_1Rs at pre- and postsynaptic sites, as observed in other brain regions (Tetzlaff et al., 1987; Ochiishi et al., 1999; Rebola et al., 2003; Rebola et al., 2005). Ochiishi et al. (1999) found A_1R expression mainly in layers 2–6 in most areas of cerebral cortex. Light and electron microscopy revealed expression in presynaptic terminals, postsynaptic membranes, and some expression in the somato-dendritic cytoplasm. They suggested that the latter might reflect active transport of A_1Rs to synaptic membranes. Thus, the combined ISH and IHC results suggest that *Adora1* transcripts are concentrated in the somatic cytoplasm, while the translated receptor proteins are transported to cell membranes (Fig. 20). These expression patterns raise several questions about A_1R-adenosine signaling in A1.

First, what are the roles of A_1Rs in the cortico-cortical and cortico-fugal projections of A1 neurons? Neurons in L3/L5/L6 project to a wide range of cortical and subcortical targets (Fig. 20). Briefly, neurons in L6, which had the highest *Adora1* expression levels, project to MG and IC, and receive inputs from the MG and cortical neurons in other locations. Neurons in L5 have widespread subcortical, corticocortical, or callosal projections, depending on the subpopulation. Neurons in L4 receive dense projections from the MG and have largely local projections. L3 neurons also receive thalamic inputs, and have local and longer range corticocortical and callosal projections. Is presynaptic A_1R-adenosine signaling also involved in regulating glutamate release in *all* of these projections? It may be significant that while plasticity becomes gated at

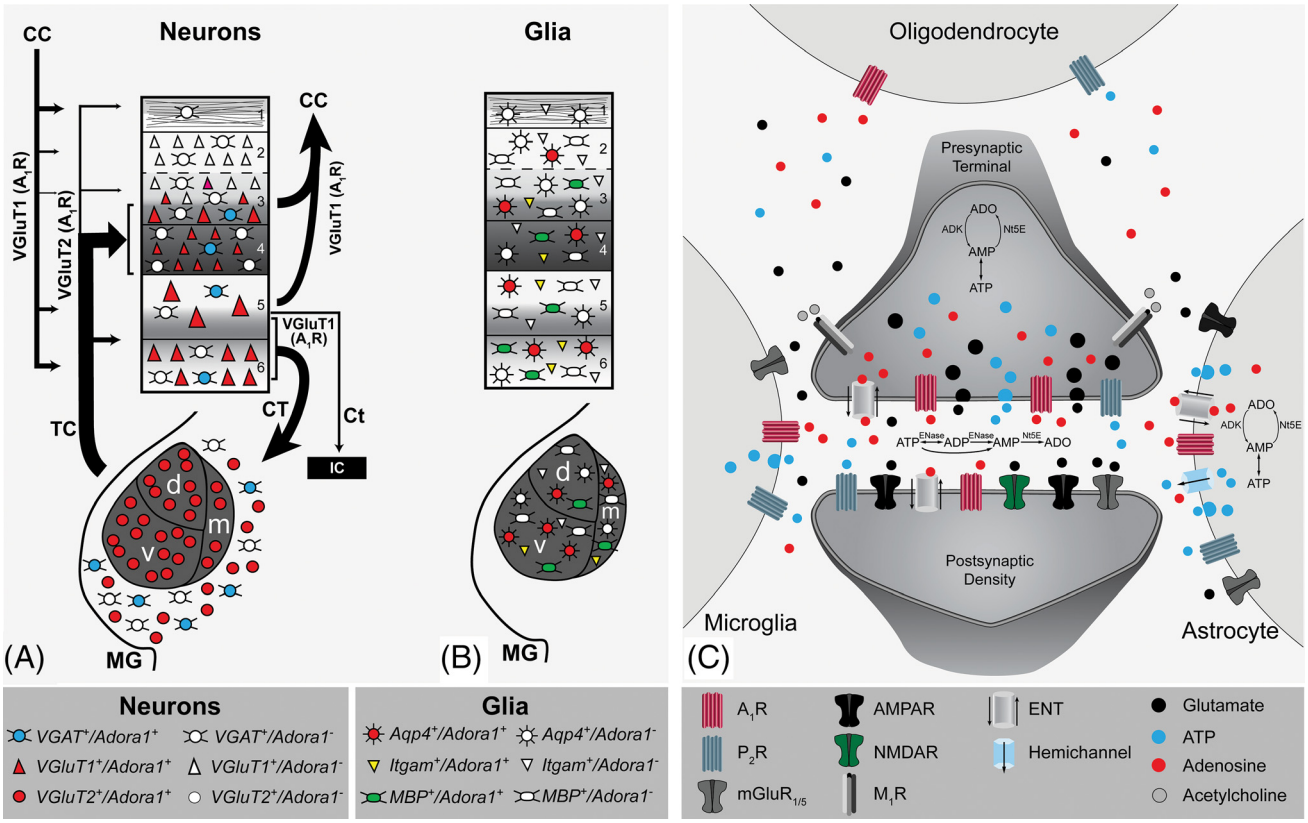

Fig. 20. Schematic summaries of *Adora1* mRNA expression in the auditory forebrain (left) and adenosine signaling at a glutamatergic synapse (right). Symbol keys for A–C below each panel. (**A**) *Adora1* expression by glutamatergic (triangles) and GABAergic (circles) neurons in A1 and MG. Filled symbols denote *Adora1*$^+$ cells. White fill, *Adora1*$^-$. Arrows summarize thalamocortical (TC), corticocortical (CC), corticothalamic (CT), and corticotectal (Ct) projections of VGluT1/A_1R and VGluT2/A_1R containing neurons in A1 and MG. Line thickness corresponds to projection strength. Background shading in A1 layers represents relative density of VGluT2/A_1R TC inputs from MG (Hackett et al., 2016). (**B**) *Adora1* expression by astrocytes (circles), oligodendrocytes (ovals), and microglia (triangles) in A1 and MG. Filled symbols denote *Adora1*$^+$ cells. White fill, *Adora1*$^-$. (**C**) Schematic highlighting basic elements of adenosine signaling at a glutamatergic synapse. Adenosine (ADO, red circles) and ATP (blue circles) are released mainly by neurons, astrocytes, and/or microglia by several mechanisms, including exocytosis and translocation through equilibrative nucleoside transporters (ENTs) and connexin/pannexin hemichannels. Intracellular adenosine levels are controlled by a cycle involving adenosine kinase (ADK) and ecto-5′-nucleotidase (Nt5E). Extracellular adenosine levels are regulated *via* catabolism of ATP by ectonucleotidases (ENase, Nt5E). Adenosine (A_1R) and ATP (P_2 class) receptors occupy pre- and postsynaptic neuronal membranes, astrocytes, microglia, and oligodendrocytes. Cholinergic binding of presynaptic M_1 acetylcholine receptors interferes with A_1R signaling, permitting sustained glutamate release. Group 1 mGluRs mediate LTP and LTD in TC projections. Model compiled from present and prior studies reviewed in the Discussion. For simplicity, only the most relevant signaling cascades and receptors are included. Some details may vary by brain region and cell type, and are subject to later revision.

mature TC synapses, cortico-cortical synapses remain plastic after critical periods close (Amitai, 2001; Froemke et al., 2007; Jiang et al., 2007; Oswald and Reyes, 2008, 2011; Huang et al., 2012), suggesting different regulatory mechanisms for TC and CC projections. Indeed, whereas interference with A_1R-adenosine signaling in MG was sufficient to restore cortical map plasticity, the same manipulations at corticocortical synapses in A1 were not (Blundon et al., 2017). The reasons remain unknown. Thus, presynaptic A_1R-adenosine gating may be specific to TC projections, but have other functions in CC or corticofugal projections.

Second, what is the significance of different *Adora1* expression levels between neurons or across cortical layers? *Adora1* was widely expressed by glutamatergic neurons in L3–L6, but levels varied significantly between layers in A1, the belt areas bordering A1 (AuV, AuD), and in the cortical domains of other sensory modalities (Fig. 2), suggesting functional homologies among sensory cortical areas. Unfortunately, the precise nature of the relationship between transcript and receptor density in different cellular compartments is not straightforward. In addition to variation in the regulation of transcription or translation, mRNA transcripts and proteins may be localized to different subcellular compartments. For example, studies in hippocampus identified a mismatch between *Adora1* mRNA and A_1R protein expression, largely explained by the fact that A_1Rs are concentrated in presynaptic terminals located in brain regions distant from their mRNA-containing somata (Johansson et al., 1993; Swanson et al., 1995). In this study, *Adora1* mRNA expression was highest in neuronal somata of L6, followed by L3/L4, whereas punctate A_1R immunoreactivity was highest in L3/L4, followed by L6, consistent with findings in several species (Fastbom et al., 1987). This mismatched laminar pattern partly reflects the high

density of immunoreactive TC terminals in L3/L4 from *Adora1*$^+$ projection neurons in the MG, and naturally parallels VGluT2 expression patterns in the auditory forebrain (Hackett et al., 2016). That is, VGluT2 immunoreactive terminals are most highly expressed in L3/4, followed by L6 (similar to A_1R), and *VGluT2* and *Adora1* mRNA are co-expressed by perhaps all glutamatergic neurons in MG. Thus, there is a general correspondence in the expression patterns of *VGluT2* and *Adora1* mRNA and their associated proteins in the TC circuit, reflecting the functional link between presynaptic adenosine and glutamate (Fig. 20).

By extension, such anatomical relationships may be expected to apply to other projections. For example, *VGluT1*$^+$ neurons in L6, which have the highest *Adora1* mRNA expression in A1, are the source of a dense network of descending projections to multiple subcortical nuclei in thalamus and brainstem (Bajo et al., 1995; Winer, 2005; Bajo and King, 2012; Crandall et al., 2015; Guo et al., 2017) (Fig. 20). A reasonable prediction is that presynaptic A_1R-adenosine signaling is important in the modulatory environment of those projections, as well. Conversely, A_1R-adenosine signaling could be considered relatively less important for neurons in superficial cortical layers (e.g., L2), where *Adora1* expression is nominal. These relationships are reflected in the summary diagram of Figure 20A, where A_1R expression is contained in *VGluT1*$^+$ or *VGluT2*$^+$ neurons in corticocortical (CC), thalamocortical (TC), corticothalamic (CT), and corticotectal (Ct) projection systems in the auditory forebrain.

Third, in addition to laminar differences in expression, there was diversity among neurons within the same layers. For example, *Adora1*$^+$ puncta numbers were very high in some *VGluT1*$^+$ neurons, but not others (Fig. 6). Because the projections of neurons within the same cortical layer can vary significantly (i.e., cortico-cortical, cortico-thalamic, cortico-tectal), differences in A_1R utilization may also vary by neuronal subpopulation, perhaps in a manner related to connectivity in the network. Indeed, the anatomical and physiological characteristics of neurons in the same cortical layer are often distinct, and those differences linked to their transcriptional heterogeneity (Chevee et al., 2018). Further, *Adora1* expression was relatively low in the majority of GABAergic neurons. Roughly 20% of *VGAT*$^+$ neurons in A1 were identified as *Adora1*$^+$, but most contained just a few puncta, and higher numbers were restricted to a minor subpopulation. The identity of that subpopulation is not yet known. Functionally, the implications are not clear, as adenosine signaling has not been studied in GABAergic neurons in A1. Elsewhere in the brain (e.g., hippocampus), A_1R expression is strong in most glutatamatergic neurons, but tends to be significant only in subpopulations of GABAergic interneurons (Rivkees et al., 1995; Ochiishi et al., 1999; Zeisel et al., 2015). Accordingly, GABA release is often not influenced by activation of A_1Rs (Cunha and Ribeiro, 2000; Cristovao-Ferreira et al., 2009). However, in a specific CA1 interneuron subtype, downregulation of extrasynaptic $GABA_A$ receptors by adenosine disinhibits those GABAergic interneurons (Klausberger et al., 2005; Rombo et al., 2016). Alternatively, adenosine signaling can regulate synaptic GABA levels *via* astrocytic transport initiated by activation of A_1–A_{2a} heteromers on astrocytes (Cristovao-Ferreira et al., 2013). Thus, the impact of A_1R-mediated adenosine signaling on GABAergic inhibition in auditory forebrain may operate through such indirect mechanisms and involve particular neuronal classes.

Last, what are the impacts of postsynaptic A_1R-adenosine signaling on neurons in A1? Are the effects different for A_1Rs located on somata or dendrites? The expression patterns identified here imply that adenosine signaling *via* postsynaptic A_1 receptors could influence the activity of glutamatergic neurons in L3–L6 of auditory cortex, and perhaps a subpopulation of GABAergic cells, consistent with findings in other brain regions (Abbracchio et al., 2009; Wei et al., 2011; Lovatt et al., 2012; Dias et al., 2013). Functionally, studies conducted primarily in hippocampus indicate that the postsynaptic effects of A_1R activation typically include decreased activation of ionotropic NMDA receptors and associated cation channel conductances, while A_1R blockade has the opposite effect (Proctor and Dunwiddie, 1987; Klishin et al., 1995a; Klishin et al., 1995b; Wetherington and Lambert, 2002; Chung et al., 2009; Kim and Johnston, 2015). Moreover, these effects can vary regionally by neuronal subpopulation and A_1R expression density (Lee et al., 1983; Kim and Johnston, 2015), indicating that properties may vary by specific location or cell type. As mentioned above, induction of LTD, LTP and receptive field plasticity in auditory cortex was distinct for pre- and postsynaptic A_1Rs (Blundon et al., 2011; Chun et al., 2013; Blundon et al., 2017), highlighting potential differences in pre- or postsynaptic A_1R-adenosine signaling.

4.5 *Adora1* Expression by Glia in the Auditory Forebrain

Historically, studies of brain structure and function have emphasized characterization of neurons and neuronal networks, but interest in the roles of glia has rapidly increased (Kettenmann and Ransom, 2013). In part, this stems from evidence that glial and neuro-glial interactions are involved in a vast array of brain functions, such as regulation of synaptic transmission, plasticity, information processing, myelination, neuronal development, and response to injury. Several outstanding reviews cover various aspects of this rapidly growing field (Stevens et al., 2002; Fields and Burnstock, 2006; Boison, 2008a; Pelligrino et al., 2011; Lovatt et al., 2012; Del Puerto et al., 2013; Domercq et al., 2013; Boison and Aronica, 2015; Bynoe et al., 2015; Coppi et al., 2015; Croft et al., 2015; Koles et al., 2016). The various roles played by glia often involve bidirectional signaling between neurons and glia, or between glia (Parpura and Zorec, 2010; Araque et al., 2014; Perea et al., 2014; Croft et al., 2015). *Astrocytes*, in particular, can detect synaptic activity *via* ionotropic and metabotropic receptors, initiating changes in signaling that modulate synaptic transmission and plasticity (Ota et al., 2013; Bernardinelli et al., 2014; Chung et al., 2015; De Pitta et al., 2016). For example, Ca^{2+} signaling in astrocytes can be invoked by sensory stimulation (Wang et al., 2006; Winship et al., 2007), initiating the vesicular exocytosis of "gliotransmitters" (e.g., glutamate, ATP, adenosine, peptides) that modulate the activity of neurons and other glia. *Oligodendrocytes* are responsible for myelination during development, but even in mature cells, activity-dependent changes in myelin production may contribute to the regulation of critical periods for plasticity in sensory systems (Takesian and

Hensch, 2013). Some of these interactions are mediated by neurotransmitter receptors localized on oligodendrocytes (Garcia-Barcina and Matute, 1996; Karadottir et al., 2005; Micu et al., 2007; Bagayogo and Dreyfus, 2009), paired with release mechanisms that permit signaling back to neurons (Fruhbeis et al., 2013). *Microglia* are activated in response to traumatic injury to the brain, but in healthy tissue (not activated), their processes move about in the neuropil, surveying local conditions (Wake et al., 2013). Like astrocytes, microglia make contacts with synapses, with effects on structure and function (Wake et al., 2009; Tremblay et al., 2010), neuronal activity (Moriguchi et al., 2003; Hayashi et al., 2006), synaptic plasticity and learning (Tremblay and Majewska, 2011; Tremblay et al., 2012), and many other functions (Kettenmann et al., 2013; Morris et al., 2013). These interactions are achieved, in part, through the expression of many types of neurotransmitter receptors in several families (Pocock and Kettenmann, 2007; Kettenmann et al., 2011; Gertig and Hanisch, 2014).

Among the signaling pathways identified, purinergic signaling is a widespread mechanism for communication between neurons, glia, and vascular cells in the brain (Burnstock and Knight, 2004; Fields and Burnstock, 2006; Burnstock et al., 2011). Both ATP and adenosine can function as signals in these interactions, subserving key roles in development, behavior, regeneration, plasticity, and pathology (Stevens et al., 2002; Dale, 2008; Boison et al., 2010; Burnstock et al., 2011; Wei et al., 2011; Zimmermann, 2011; Krugel, 2016; Pedata et al., 2016). Astrocytes (and neurons) release ATP, which is converted to adenosine in the extracellular space, with impacts on both neurons and glia (Pascual et al., 2005; Lovatt et al., 2012). A major role of A_1Rs in astrocytes is to trigger the removal of excess adenosine from the synapse *via* ENTs (Boison, 2008b; Lovatt et al., 2012; Hines and Haydon, 2014), with effects on glutamatergic transmission (Masino et al., 2002) and plasticity (Navarrete et al., 2012). A_1R signaling can also mediate protective effects on astrocytes during insults such as hypoxia (Ciccarelli et al., 2007; Bjorklund et al., 2008). In oligodendrocytes, A_1Rs promote myelination during axonal maturation (Stevens et al., 2002), and contribute to white matter loss in pathology (Kim et al., 2005). In microglia, A_1R activation on microglia can regulate proliferation (Haselkorn et al., 2010), limit the inflammatory response (Tsutsui et al., 2004), contribute to the neuroprotective effects associated with adenosine delivery (Lauro et al., 2010; Pedata et al., 2016), and modulate short-term synaptic transmission and plasticity (George et al., 2016). Many other functions are mediated by purinergic signaling through other receptors and pathways, as well.

A general finding of this study was that *Adora1* is expressed by subpopulations of all three glial classes in A1 and MG (Fig. 20). Astrocytes and oligodendrocytes were more likely to express *Adora1*$^+$ puncta than microglia. Transcript abundance was much lower in glia than neurons, regardless of location, and was uniform across cortical layers in A1 or between divisions in MG (except perivascular and pial astrocytes, where *Adora1* expression was usually nominal). This pattern contrasts sharply with relatively strong *Adora1* expression by the majority of neurons.

The reasons for the differences between neurons and glia are not entirely clear, but presumably related to the specific functions mediated by A_1Rs in each cell type. Certainly, expression levels in glia are sufficient to meet functional demands, and the uniformly low transcript abundance suggests that those needs do not fluctuate widely over time or location. That is, high receptor numbers are not necessary to maintain functionality, in general, nor are high numbers needed to achieve a specialized function that might require elevated sensitivity.

For other functions, A_1R-adenosine signaling in glia may not be as important as those mediated by other purine receptors (Fields and Burnstock, 2006), several of which are significantly expressed in A1 and MG (Fig. 1). As one example, the P_2 ATP receptor, *P2ry12*, is highly expressed in microglia compared to neurons and other glia (Zhang et al., 2014; Zeisel et al., 2015), with specialized roles in the response to local brain injury (Davalos et al., 2005; Amadio et al., 2006). Much remains to be learned about purinergic signaling, in general, as this receptor family may contribute to neuron–glia interactions, and many other functions in auditory forebrain.

4.6 Subcellular Localization of Transcripts

Transcripts for the seven mRNA markers used in this study were primarily concentrated in the somatic cytoplasm, but for some markers (*MBP, Aqp4, Adora1*), labeled puncta were consistently found in the neuropil. DIC microscopy indicated that most were localized to peripheral processes. High numbers of *MBP*$^+$ transcripts were located in the peripheral processes of oligodendrocytes (presumably), consistent with numerous previous studies in other brain regions (Colman et al., 1982; Trapp et al., 1987; Verity and Campagnoni, 1988; Shiota et al., 1989; Barbarese et al., 1995; Ainger et al., 1997; Muller et al., 2013). Although some instances of labeled puncta were possibly nonspecific labeling (noise), the majority was localized to peripheral processes. Internal evidence for this conclusion derives from the high specificity of the probes, and the low levels of noise in areas with few cells (e.g., cortical layer 1).

In addition, it is well established that the transcripts of perhaps thousands of protein coding genes are localized in the neuropil, where local translation may occur (Steward and Levy, 1982; Tiruchinapalli et al., 2003; Bockers et al., 2004; Poon et al., 2006; Zhong et al., 2006; Lein et al., 2007; Giuditta et al., 2008; Cajigas et al., 2012; Sakers et al., 2017). Among the genes with significant neuropil expression in hippocampus are *Adora1*, *MBP*, *Aqp4*, *VGluT1*, and numerous neurotransmitter receptors (Cajigas et al., 2012). In a recent study focused on astrocytes, Sakers et al. (2017) showed that the machinery for local translation of transcripts is localized in their peripheral processes. RNAseq analyses of peripheral astrocyte fractions revealed modest levels of *Adora1*, *Aqp4*, and *GFAP*, suggesting some degree of transcript expression outside somata. This could be functionally significant, as a single astrocyte may contact thousands of synapses (Oberheim et al., 2006), and numerous functions may benefit from local translation. Altogether, these findings are consistent with present observations in the auditory forebrain, and suggest that peripheral transcript localization is a general property of some genes.

4.7 Transcript Abundance

Relevant to the subject of transcript localization is the relationship between transcript and protein abundance. Within a cellular compartment, such as the somatic cytoplasm or peripheral process, how many transcripts constitute a functionally significant number? For somata, we took a conservative approach in setting the threshold to three or more copies. This threshold was somewhat arbitrary, and may under- or over-represent cells that in fact produce significant amounts of functional protein. Moreover, our approach excluded transcripts located beyond somata within peripheral processes. Indeed, the presence of single transport granules containing mRNA (along with ribosome and other molecules) appears to be sufficient for local translation in the peripheral processes of oligodendrocytes (e.g., myelin basic protein) (Muller et al., 2013).

Unfortunately, correlations between transcript and protein abundance are variable, and tend to be modest on average (Ghazalpour et al., 2011; Vogel and Marcotte, 2012). Factors contributing to the variability include regulation of transcription and translation, transcript stability, and protein degradation, as well as methodological limitations. Thus, the relationship between transcript copy number in the cytoplasm and protein expression levels in the cytoplasm or elsewhere in the cell is not clear for a given target. As mentioned above, the relationship between transcripts and translated proteins may be further complicated in neurons for which transcripts are concentration in somatic cytoplasm, but the proteins are expressed in a different subcellular compartment, such as axon terminals. This is the case for VGluT1, VGluT2, and VGAT (Hackett et al., 2016), as well as A_1Rs.

4.8 Summary

The findings of this study are summarized in Figure 20. The main findings for neurons were that *Adora1* mRNA is strongly expressed by the majority of glutamatergic neurons in layers 3–6 of A1 and all divisions of the MG, compared to modest expression by subpopulations of GABAergic neurons in A1. A_1R immunoreactivity was also found across layers, but peak expression corresponded with bands of elevated VGluT2 expression in L3/L4 and L6. These patterns indicate that A_1Rs are likely co-expressed with VGluT1 or VGluT2 in axon terminals of respective glutamatergic projections. For glia, *Adora1* mRNA is expressed by subpopulations of all three glial subtypes in L3–L6 of A1 and all divisions of MG, but transcript abundance is low compared to neurons.

The widespread *Adora1* expression by MG neurons implies that the presynaptic modulation of glutamate release by adenosine may be a general property of all MG projections to auditory cortex, and therefore potentially impact excitatory neurotransmission and plasticity in all areas of auditory cortex. As A_1R functionality in auditory cortical neurons appears to be distinct from MG neurons, focused studies will be needed to uncover the roles of pre- and postsynaptic receptors in the networks of corticocortical (CC), corticothalamic (CT), and corticotectal (Ct) projections. The expression of *Adora1* by glial subpopulations is consistent with recognized roles in development, behavior, regeneration, plasticity, and pathology, but specific roles in the auditory forebrain are unknown.

An added application of the data from this study concerns the targeting of specific cell types for future functional studies, as the properties of A_1R-adenosine signaling in the auditory forebrain are currently limited to a subset of the TC projections from MGv to L4 of A1. Gene editing, transgenic, optogenetic, and pharmacologic manipulations of A_1R-mediated signaling would be expected to differentially impact subpopulations of neurons and glia in A1 and MG. Strategies to target *Adora1* or A_1Rs in specific cell populations for experimental study of function can be developed from the data generated here.

Literature Cited

Abbracchio MP, Burnstock G, Verkhratsky A, Zimmermann H. 2009. Purinergic signalling in the nervous system: an overview. Trends Neurosci 32:19–29.

Ainger K, Avossa D, Diana AS, Barry C, Barbarese E, Carson JH. 1997. Transport and localization elements in myelin basic protein mRNA. J Cell Biol 138:1077–1087.

Alghamdi B, Fern R. 2015. Phenotype overlap in glial cell populations: astroglia, oligodendroglia and NG-2(+) cells. Front Neuroanat 9:49.

Amadio S, Tramini G, Martorana A, Viscomi MT, Sancesario G, Bernardi G, Volonte C. 2006. Oligodendrocytes express P2Y12 metabotropic receptor in adult rat brain. Neuroscience 141: 1171–1180.

Amitai Y. 2001. Thalamocortical synaptic connections: efficacy, modulation, inhibition and plasticity. Rev Neurosci 12:159–173.

Anderson LA, Linden JF. 2011. Physiological differences between histologically defined subdivisions in the mouse auditory thalamus. Hear Res 274:48–60.

Anderson LA, Christianson GB, Linden JF. 2009. Mouse auditory cortex differs from visual and somatosensory cortices in the laminar distribution of cytochrome oxidase and acetylcholinesterase. Brain Res 1252:130–142.

Aoyama M, Kakita H, Kato S, Tomita M, Asai K. 2012. Region-specific expression of a water channel protein, aquaporin 4, on brain astrocytes. J Neurosci Res 90:2272–2280.

Araque A, Carmignoto G, Haydon PG, Oliet SH, Robitaille R, Volterra A. 2014. Gliotransmitters travel in time and space. Neuron 81:728–739.

Baalman K, Marin MA, Ho TS, Godoy M, Cherian L, Robertson C, Rasband MN. 2015. Axon initial segment-associated microglia. J Neurosci 35:2283–2292.

Badaut J, Lasbennes F, Magistretti PJ, Regli L. 2002. Aquaporins in brain: distribution, physiology, and pathophysiology. J Cereb Blood Flow Metab 22:367–378.

Bagayogo IP, Dreyfus CF. 2009. Regulated release of BDNF by cortical oligodendrocytes is mediated through metabotropic glutamate receptors and the PLC pathway. ASN Neuro 1(1). pii: e00001. doi: 10.1042/AN20090006.

Bajo VM, King AJ. 2012. Cortical modulation of auditory processing in the midbrain. Front Neural Circuit 6:114.

Bajo VM, Rouiller EM, Welker E, Clarke S, Villa AE, de Ribaupierre Y, de Ribaupierre F. 1995. Morphology and spatial distribution of corticothalamic terminals originating from the cat auditory cortex. Hear Res 83:161–174.

Bao S, Chang EF, Davis JD, Gobeske KT, Merzenich MM. 2003. Progressive degradation and subsequent refinement of acoustic representations in the adult auditory cortex. J Neurosci 23: 10765–10775.

Barbarese E, Koppel DE, Deutscher MP, Smith CL, Ainger K, Morgan F, Carson JH. 1995. Protein translation components are colocalized in granules in oligodendrocytes. J Cell Sci 108(Pt 8): 2781–2790.

Barkat TR, Polley DB, Hensch TK. 2011. A critical period for auditory thalamocortical connectivity. Nat Neurosci 14:1189–1194.
Barroso-Chinea P, Castle M, Aymerich MS, Perez-Manso M, Erro E, Tunon T, Lanciego JL. 2007. Expression of the mRNAs encoding for the vesicular glutamate transporters 1 and 2 in the rat thalamus. J Comp Neurol 501:703–715.
Bavelier D, Levi DM, Li RW, Dan Y, Hensch TK. 2010. Removing brakes on adult brain plasticity: from molecular to behavioral interventions. J Neurosci 30:14964–14971.
Bayazitov IT, Richardson RJ, Fricke RG, Zakharenko SS. 2007. Slow presynaptic and fast postsynaptic components of compound long-term potentiation. J Neurosci 27:11510–11521.
Bernardinelli Y, Muller D, Nikonenko I. 2014. Astrocyte-synapse structural plasticity. Neural Plast 2014:232105.
Bjorklund O, Shang M, Tonazzini I, Dare E, Fredholm BB. 2008. Adenosine A1 and A3 receptors protect astrocytes from hypoxic damage. Eur J Pharmacol 596:6–13.
Blake DT, Strata F, Churchland AK, Merzenich MM. 2002. Neural correlates of instrumental learning in primary auditory cortex. Proc Natl Acad Sci U S A 99:10114–10119.
Blundon JA, Zakharenko SS. 2013. Presynaptic gating of postsynaptic synaptic plasticity: a plasticity filter in the adult auditory cortex. Neuroscientist 19:465–478.
Blundon JA, Bayazitov IT, Zakharenko SS. 2011. Presynaptic gating of postsynaptically expressed plasticity at mature thalamocortical synapses. J Neurosci 31:16012–16025.
Blundon JA, Roy NC, Teubner BJW, Yu J, Eom TY, Sample KJ, Pani A, Smeyne RJ, Han SB, Kerekes RA, et al. 2017. Restoring auditory cortex plasticity in adult mice by restricting thalamic adenosine signaling. Science 356:1352–1356.
Bockers TM, Segger-Junius M, Iglauer P, Bockmann J, Gundelfinger ED, Kreutz MR, Richter D, Kindler S, Kreienkamp HJ. 2004. Differential expression and dendritic transcript localization of Shank family members: identification of a dendritic targeting element in the 3′ untranslated region of Shank1 mRNA. Mol Cell Neurosci 26:182–190.
Boison D. 2006. Adenosine kinase, epilepsy and stroke: mechanisms and therapies. Trends Pharmacol Sci 27:652–658.
Boison D. 2008a. Adenosine as a neuromodulator in neurological diseases. Curr Opin Pharmacol 8:2–7.
Boison D. 2008b. The adenosine kinase hypothesis of epileptogenesis. Prog Neurobiol 84:249–262.
Boison D. 2013. Adenosine kinase: exploitation for therapeutic gain. Pharmacol Rev 65:906–943.
Boison D, Aronica E. 2015. Comorbidities in neurology: is adenosine the common link? Neuropharmacology 97:18–34.
Boison D, Chen JF, Fredholm BB. 2010. Adenosine signaling and function in glial cells. Cell Death Differ 17:1071–1082.
Brundege JM, Dunwiddie TV. 1996. Modulation of excitatory synaptic transmission by adenosine released from single hippocampal pyramidal neurons. J Neurosci 16:5603–5612.
Burke TM, Markwald RR, McHill AW, Chinoy ED, Snider JA, Bessman SC, Jung CM, O'Neill JS, Wright KP Jr. 2015. Effects of caffeine on the human circadian clock in vivo and in vitro. Sci Transl Med 7:305ra146.
Burnstock G. 2007. Physiology and pathophysiology of purinergic neurotransmission. Physiol Rev 87:659–797.
Burnstock G, Knight GE. 2004. Cellular distribution and functions of P2 receptor subtypes in different systems. Int Rev Cytol 240: 31–304.
Burnstock G, Krugel U, Abbracchio MP, Illes P. 2011. Purinergic signalling: from normal behaviour to pathological brain function. Prog Neurobiol 95:229–274.
Buttini M, Yu GQ, Shockley K, Huang Y, Jones B, Masliah E, Mallory M, Yeo T, Longo FM, Mucke L. 2002. Modulation of Alzheimer-like synaptic and cholinergic deficits in transgenic mice by human apolipoprotein E depends on isoform, aging, and overexpression of amyloid beta peptides but not on plaque formation. J Neurosci 22:10539–10548.
Bynoe MS, Viret C, Yan A, Kim DG. 2015. Adenosine receptor signaling: a key to opening the blood-brain door. Fluids Barriers CNS 12:20.
Cahoy JD, Emery B, Kaushal A, Foo LC, Zamanian JL, Christopherson KS, Xing Y, Lubischer JL, Krieg PA, Krupenko SA, et al. 2008. A transcriptome database for astrocytes, neurons, and oligodendrocytes: a new resource for understanding brain development and function. J Neurosci 28:264–278.
Cajigas IJ, Tushev G, Will TJ, tom Dieck S, Fuerst N, Schuman EM. 2012. The local transcriptome in the synaptic neuropil revealed by deep sequencing and high-resolution imaging. Neuron 74: 453–466.
Chaudhry FA, Reimer RJ, Bellocchio EE, Danbolt NC, Osen KK, Edwards RH, Storm-Mathisen J. 1998. The vesicular GABA transporter, VGAT, localizes to synaptic vesicles in sets of glycinergic as well as GABAergic neurons. J Neurosci 18:9733–9750.
Chen JF, Lee CF, Chern Y. 2014. Adenosine receptor neurobiology: overview. Int Rev Neurobiol 119:1–49.
Chevee M, Robertson JJ, Cannon GH, Brown SP, Goff LA. 2018. Variation in activity state, axonal projection, and position define the transcriptional identity of individual neocortical projection neurons. Cell Rep 22:441–455.
Chun S, Bayazitov IT, Blundon JA, Zakharenko SS. 2013. Thalamocortical long-term potentiation becomes gated after the early critical period in the auditory cortex. J Neurosci 33:7345–7357.
Chung HJ, Ge WP, Qian X, Wiser O, Jan YN, Jan LY. 2009. G protein-activated inwardly rectifying potassium channels mediate depotentiation of long-term potentiation. Proc Natl Acad Sci U S A 106:635–640.
Chung WS, Allen NJ, Eroglu C. 2015. Astrocytes control synapse formation, function, and elimination. Cold Spring Harb Perspect Biol 7:a020370.
Ciccarelli R, D'Alimonte I, Ballerini P, D'Auro M, Nargi E, Buccella S, Di Iorio P, Bruno V, Nicoletti F, Caciagli F. 2007. Molecular signalling mediating the protective effect of A1 adenosine and mGlu3 metabotropic glutamate receptor activation against apoptosis by oxygen/glucose deprivation in cultured astrocytes. Mol Pharmacol 71:1369–1380.
Colman DR, Kreibich G, Frey AB, Sabatini DD. 1982. Synthesis and incorporation of myelin polypeptides into CNS myelin. J Cell Biol 95:598–608.
Coppi E, Cellai L, Maraula G, Dettori I, Melani A, Pugliese AM, Pedata F. 2015. Role of adenosine in oligodendrocyte precursor maturation. Front Cell Neurosci 9:155.
Crair MC, Malenka RC. 1995. A critical period for long-term potentiation at thalamocortical synapses. Nature 375:325–328.
Crandall SR, Cruikshank SJ, Connors BW. 2015. A corticothalamic switch: controlling the thalamus with dynamic synapses. Neuron 86:768–782.
Cristovao-Ferreira S, Vaz SH, Ribeiro JA, Sebastiao AM. 2009. Adenosine A2A receptors enhance GABA transport into nerve terminals by restraining PKC inhibition of GAT-1. J Neurochem 109: 336–347.
Cristovao-Ferreira S, Navarro G, Brugarolas M, Perez-Capote K, Vaz SH, Fattorini G, Conti F, Lluis C, Ribeiro JA, McCormick PJ, et al. 2013. A_1R-A2AR heteromers coupled to Gs and G i/0 proteins modulate GABA transport into astrocytes. Purinergic Signal 9: 433–449.
Croft W, Dobson KL, Bellamy TC. 2015. Plasticity of neuron-glial transmission: equipping glia for long-term integration of network activity. Neural Plast 2015:765792.
Cruikshank SJ, Killackey HP, Metherate R. 2001. Parvalbumin and calbindin are differentially distributed within primary and secondary subregions of the mouse auditory forebrain. Neuroscience 105: 553–569.
Cunha RA. 2001. Adenosine as a neuromodulator and as a homeostatic regulator in the nervous system: different roles, different sources and different receptors. Neurochem Int 38:107–125.
Cunha RA. 2016. How does adenosine control neuronal dysfunction and neurodegeneration? J Neurochem 139:1019–1055.
Cunha RA, Ribeiro JA. 2000. Purinergic modulation of [(3)H]GABA release from rat hippocampal nerve terminals. Neuropharmacology 39:1156–1167.
Dale N. 2008. Dynamic ATP signalling and neural development. J Physiol 586:2429–2436.

Davalos D, Grutzendler J, Yang G, Kim JV, Zuo Y, Jung S, Littman DR, Dustin ML, Gan WB. 2005. ATP mediates rapid microglial response to local brain injury in vivo. Nat Neurosci 8:752–758.

De Pitta M, Brunel N, Volterra A. 2016. Astrocytes: orchestrating synaptic plasticity? Neuroscience 323:43–61.

de Villers-Sidani E, Chang EF, Bao S, Merzenich MM. 2007. Critical period window for spectral tuning defined in the primary auditory cortex (A1) in the rat. J Neurosci 27:180–189.

Del Puerto A, Wandosell F, Garrido JJ. 2013. Neuronal and glial purinergic receptors functions in neuron development and brain disease. Front Cell Neurosci 7:197.

Dias RB, Rombo DM, Ribeiro JA, Henley JM, Sebastiao AM. 2013. Adenosine: setting the stage for plasticity. Trends Neurosci 36: 248–257.

Domercq M, Vazquez-Villoldo N, Matute C. 2013. Neurotransmitter signaling in the pathophysiology of microglia. Front Cell Neurosci 7:49.

Dumoulin A, Rostaing P, Bedet C, Levi S, Isambert MF, Henry JP, Triller A, Gasnier B. 1999. Presence of the vesicular inhibitory amino acid transporter in GABAergic and glycinergic synaptic terminal boutons. J Cell Sci 112(Pt 6):811–823.

Dunwiddie TV, Masino SA. 2001. The role and regulation of adenosine in the central nervous system. Annu Rev Neurosci 24:31–55.

Edeline JM. 2003. The thalamo-cortical auditory receptive fields: regulation by the states of vigilance, learning and the neuromodulatory systems. Exp Brain Res 153:554–572.

Edeline JM. 2012. Beyond traditional approaches to understanding the functional role of neuromodulators in sensory cortices. Front Behav Neurosci 6:45.

Evans CF, Horwitz MS, Hobbs MV, Oldstone MB. 1996. Viral infection of transgenic mice expressing a viral protein in oligodendrocytes leads to chronic central nervous system autoimmune disease. J Exp Med 184:2371–2384.

Fastbom J, Pazos A, Palacios JM. 1987. The distribution of adenosine A1 receptors and 5′-nucleotidase in the brain of some commonly used experimental animals. Neuroscience 22:813–826.

Ferrati G, Martini FJ, Maravall M. 2016. Presynaptic adenosine receptor-mediated regulation of diverse thalamocortical short-term plasticity in the mouse whisker pathway. Front Neural Circuit 10:9.

Fields RD, Burnstock G. 2006. Purinergic signalling in neuron-glia interactions. Nat Rev Neurosci 7:423–436.

Fontanez DE, Porter JT. 2006. Adenosine A1 receptors decrease thalamic excitation of inhibitory and excitatory neurons in the barrel cortex. Neuroscience 137:1177–1184.

Franklin BJ, Paxinos G. 2007. *The mouse brain in stereotaxic coordinates*. New York, NY: Academic Press.

Fredholm BB. 2007. Adenosine, an endogenous distress signal, modulates tissue damage and repair. Cell Death Differ 14:1315–1323.

Fredholm BB. 2012. Rethinking the purinergic neuron-glia connection. Proc Natl Acad Sci U S A 109:5913–5914.

Fredholm BB, Dunwiddie TV. 1988. How does adenosine inhibit transmitter release? Trends Pharmacol Sci 9:130–134.

Fredholm BB, Hedqvist P. 1980. Modulation of neurotransmission by purine nucleotides and nucleosides. Biochem Pharmacol 29: 1635–1643.

Fredholm BB, Chen JF, Cunha RA, Svenningsson P, Vaugeois JM. 2005. Adenosine and brain function. Int Rev Neurobiol 63:191–270.

Fremeau RT, Kam K, Qureshi T, Johnson J, Copenhagen DR, Storm-Mathisen J, Chaudhry FA, Nicoll RA, Edwards RH. 2004. Vesicular glutamate transporters 1 and 2 target to functionally distinct synaptic release sites. Science 304:1815–1819.

Fritz JB, Elhilali M, David SV, Shamma SA. 2007. Auditory attention--focusing the searchlight on sound. Curr Opin Neurobiol 17:437–455.

Froemke RC, Jones BJ. 2011. Development of auditory cortical synaptic receptive fields. Neurosci Biobehav Rev 35:2105–2113.

Froemke RC, Merzenich MM, Schreiner CE. 2007. A synaptic memory trace for cortical receptive field plasticity. Nature 450:425–429.

Fruhbeis C, Frohlich D, Kuo WP, Amphornrat J, Thilemann S, Saab AS, Kirchhoff F, Mobius W, Goebbels S, Nave KA, et al. 2013. Neurotransmitter-triggered transfer of exosomes mediates oligodendrocyte-neuron communication. PLoS Biol 11:e1001604.

Garcia N, Priego M, Obis T, Santafe MM, Tomas M, Besalduch N, Lanuza MA, Tomas J. 2013. Adenosine A(1) and A(2)A receptor-mediated modulation of acetylcholine release in the mice neuromuscular junction. Eur J Neurosci 38:2229–2241.

Garcia-Barcina JM, Matute C. 1996. Expression of kainate-selective glutamate receptor subunits in glial cells of the adult bovine white matter. Eur J Neurosci 8:2379–2387.

George J, Cunha RA, Mulle C, Amedee T. 2016. Microglia-derived purines modulate mossy fibre synaptic transmission and plasticity through P2X4 and A1 receptors. Eur J Neurosci 43: 1366–1378.

Gertig U, Hanisch UK. 2014. Microglial diversity by responses and responders. Front Cell Neurosci 8:101.

Ghazalpour A, Bennett B, Petyuk VA, Orozco L, Hagopian R, Mungrue IN, Farber CR, Sinsheimer J, Kang HM, Furlotte N, et al. 2011. Comparative analysis of proteome and transcriptome variation in mouse. PLoS Genet 7:e1001393.

Giuditta A, Chun JT, Eyman M, Cefaliello C, Bruno AP, Crispino M. 2008. Local gene expression in axons and nerve endings: the glia-neuron unit. Physiol Rev 88:515–555.

Guo Y, Zhang P, Sheng Q, Zhao S, Hackett TA. 2016. lncRNA expression in the auditory forebrain during postnatal development. Gene 593:201–216.

Guo W, Clause AR, Barth-Maron A, Polley DB. 2017. A corticothalamic circuit for dynamic switching between feature detection and discrimination. Neuron 95(180–194):e185.

Hackett TA, Barkat TR, O'Brien BM, Hensch TK, Polley DB. 2011a. Linking topography to tonotopy in the mouse auditory thalamocortical circuit. J Neurosci 31:2983–2995.

Hackett TA, Takahata T, Balaram P. 2011b. VGLUT1 and VGLUT2 mRNA expression in the primate auditory pathway. Hear Res 274: 129–141.

Hackett TA, Guo Y, Clause A, Hackett NJ, Garbett K, Zhang P, Polley DB, Mirnics K. 2015. Transcriptional maturation of the mouse auditory forebrain. BMC Genomics 16:606.

Hackett TA, Clause AR, Takahata T, Hackett NJ, Polley DB. 2016. Differential maturation of vesicular glutamate and GABA transporter expression in the mouse auditory forebrain during the first weeks of hearing. Brain Struct Funct 221:2619–2673.

Haselkorn ML, Shellington DK, Jackson EK, Vagni VA, Janesko-Feldman K, Dubey RK, Gillespie DG, Cheng D, Bell MJ, Jenkins LW, et al. 2010. Adenosine A1 receptor activation as a brake on the microglial response after experimental traumatic brain injury in mice. J Neurotrauma 27:901–910.

Hayashi Y, Ishibashi H, Hashimoto K, Nakanishi H. 2006. Potentiation of the NMDA receptor-mediated responses through the activation of the glycine site by microglia secreting soluble factors. GLIA 53:660–668.

Hines DJ, Haydon PG. 2014. Astrocytic adenosine: from synapses to psychiatric disorders. Philos Trans R Soc Lond Ser B Biol Sci 369: 20130594.

Holt LM, Olsen ML. 2016. Novel applications of magnetic cell sorting to analyze cell-type specific gene and protein expression in the central nervous system. PLoS One 11:e0150290.

Housley GD, Bringmann A, Reichenbach A. 2009. Purinergic signaling in special senses. Trends Neurosci 32:128–141.

Hsu MS, Seldin M, Lee DJ, Seifert G, Steinhauser C, Binder DK. 2011. Laminar-specific and developmental expression of aquaporin-4 in the mouse hippocampus. Neuroscience 178:21–32.

Huang S, Trevino M, He K, Ardiles A, Pasquale R, Guo Y, Palacios A, Huganir R, Kirkwood A. 2012. Pull-push neuromodulation of LTP and LTD enables bidirectional experience-induced synaptic scaling in visual cortex. Neuron 73:497–510.

Hubbard JA, Hsu MS, Seldin MM, Binder DK. 2015. Expression of the astrocyte water channel aquaporin-4 in the mouse brain. ASN Neuro 7:175909141560548.

Insanally MN, Kover H, Kim H, Bao S. 2009. Feature-dependent sensitive periods in the development of complex sound representation. J Neurosci 29:5456–5462.

Ito T, Oliver DL. 2010. Origins of glutamatergic terminals in the inferior colliculus identified by retrograde transport and expression of VGLUT1 and VGLUT2 genes. Front Neuroanat 4:1–11.

Ito T, Bishop DC, Oliver DL. 2011. Expression of glutamate and inhibitory amino acid vesicular transporters in the rodent auditory brainstem. J Comp Neurol 519:316–340.

Jafari MR, Zhang Y, Yan J. 2007. Multiparametric changes in the receptive field of cortical auditory neurons induced by thalamic activation in the mouse. Cereb Cortex 17:71–80.

Jiang B, Trevino M, Kirkwood A. 2007. Sequential development of long-term potentiation and depression in different layers of the mouse visual cortex. J Neurosci 27:9648–9652.

Johansson B, Ahlberg S, van der Ploeg I, Brene S, Lindefors N, Persson H, Fredholm BB. 1993. Effect of long term caffeine treatment on A1 and A2 adenosine receptor binding and on mRNA levels in rat brain. Naunyn Schmiedeberg's Arch Pharmacol 347: 407–414.

Jones EG. 2007. *The Thalamus*. Cambridge: Cambridge University Press.

Kaneko T, Fujiyama F. 2002. Complementary distribution of vesicular glutamate transporters in the central nervous system. Neurosci Res 42:243–250.

Karadottir R, Cavelier P, Bergersen LH, Attwell D. 2005. NMDA receptors are expressed in oligodendrocytes and activated in ischaemia. Nature 438:1162–1166.

Keeling MD, Calhoun BM, Kruger K, Polley DB, Schreiner CE. 2008. Spectral integration plasticity in cat auditory cortex induced by perceptual training. Exp Brain Res 184:493–509.

Kettenmann H, Ransom BR. 2013. *Neuroglia*. Oxford: Oxford University Press.

Kettenmann H, Hanisch UK, Noda M, Verkhratsky A. 2011. Physiology of microglia. Physiol Rev 91:461–553.

Kettenmann H, Kirchhoff F, Verkhratsky A. 2013. Microglia: new roles for the synaptic stripper. Neuron 77:10–18.

Kim CS, Johnston D. 2015. A1 adenosine receptor-mediated GIRK channels contribute to the resting conductance of CA1 neurons in the dorsal hippocampus. J Neurophysiol 113:2511–2523.

Kim M, Yu ZX, Fredholm BB, Rivkees SA. 2005. Susceptibility of the developing brain to acute hypoglycemia involving A1 adenosine receptor activation. Am J Physiol Endocrinol Metab 289: E562–E569.

Kimura M, Saitoh N, Takahashi T. 2003. Adenosine A (1) receptor-mediated presynaptic inhibition at the calyx of Held of immature rats. J Physiol 553:415–426.

Klausberger T, Marton LF, O'Neill J, Huck JH, Dalezios Y, Fuentealba P, Suen WY, Papp E, Kaneko T, Watanabe M, et al. 2005. Complementary roles of cholecystokinin- and parvalbumin-expressing GABAergic neurons in hippocampal network oscillations. J Neurosci 25:9782–9793.

Klishin A, Lozovaya N, Krishtal O. 1995a. A1 adenosine receptors differentially regulate the N-methyl-D-aspartate and non-N-methyl-D-aspartate receptor-mediated components of hippocampal excitatory postsynaptic current in a Ca2+/Mg(2 +)-dependent manner. Neuroscience 65:947–953.

Klishin A, Tsintsadze T, Lozovaya N, Krishtal O. 1995b. Latent N-methyl-D-aspartate receptors in the recurrent excitatory pathway between hippocampal CA1 pyramidal neurons: Ca(2 +)-dependent activation by blocking A1 adenosine receptors. Proc Natl Acad Sci U S A 92:12431–12435.

Klyuch BP, Dale N, Wall MJ. 2012. Deletion of ecto-5′-nucleotidase (CD73) reveals direct action potential-dependent adenosine release. J Neurosci 32:3842–3847.

Koles L, Kato E, Hanuska A, Zadori ZS, Al-Khrasani M, Zelles T, Rubini P, Illes P. 2016. Modulation of excitatory neurotransmission by neuronal/glial signalling molecules: interplay between purinergic and glutamatergic systems. Purinergic Signal 12:1–24.

Krugel U. 2016. Purinergic receptors in psychiatric disorders. Neuropharmacology 104:212–225.

Lalo U, Palygin O, Rasooli-Nejad S, Andrew J, Haydon PG, Pankratov Y. 2014. Exocytosis of ATP from astrocytes modulates phasic and tonic inhibition in the neocortex. PLoS Biol 12: e1001747.

Lauro C, Cipriani R, Catalano M, Trettel F, Chece G, Brusadin V, Antonilli L, van Rooijen N, Eusebi F, Fredholm BB, et al. 2010. Adenosine A1 receptors and microglial cells mediate CX3CL1-induced protection of hippocampal neurons against Glu-induced death. Neuropsychopharmacology 35:1550–1559.

Lee KS, Schubert P, Reddington M, Kreutzberg GW. 1983. Adenosine receptor density and the depression of evoked neuronal activity in the rat hippocampus in vitro. Neurosci Lett 37:81–85.

Lein ES, Hawrylycz MJ, Ao N, Ayres M, Bensinger A, Bernard A, Boe AF, Boguski MS, Brockway KS, Byrnes EJ, et al. 2007. Genome-wide atlas of gene expression in the adult mouse brain. Nature 445:168–176.

Lloyd HG, Lindstrom K, Fredholm BB. 1993. Intracellular formation and release of adenosine from rat hippocampal slices evoked by electrical stimulation or energy depletion. Neurochem Int 23: 173–185.

Lovatt D, Xu Q, Liu W, Takano T, Smith NA, Schnermann J, Tieu K, Nedergaard M. 2012. Neuronal adenosine release, and not astrocytic ATP release, mediates feedback inhibition of excitatory activity. Proc Natl Acad Sci U S A 109:6265–6270.

Lu E, Llano DA, Sherman SM. 2009. Different distributions of calbindin and calretinin immunostaining across the medial and dorsal divisions of the mouse medial geniculate body. Hear Res 257: 16–23.

Ma X, Suga N. 2009. Specific and nonspecific plasticity of the primary auditory cortex elicited by thalamic auditory neurons. J Neurosci 29:4888–4896.

Manzoni OJ, Manabe T, Nicoll RA. 1994. Release of adenosine by activation of NMDA receptors in the hippocampus. Science 265: 2098–2101.

Marquez-Legorreta E, Horta-Junior Jde A, Berrebi AS, Saldana E. 2016. Organization of the zone of transition between the pretectum and the thalamus, with emphasis on the pretectothalamic lamina. Front Neuroanat 10:82.

Masino SA, Diao L, Illes P, Zahniser NR, Larson GA, Johansson B, Fredholm BB, Dunwiddie TV. 2002. Modulation of hippocampal glutamatergic transmission by ATP is dependent on adenosine a (1) receptors. J Pharmacol Exp Ther 303:356–363.

Melani A, Corti F, Stephan H, Muller CE, Donati C, Bruni P, Vannucchi MG, Pedata F. 2012. Ecto-ATPase inhibition: ATP and adenosine release under physiological and ischemic in vivo conditions in the rat striatum. Exp Neurol 233:193–204.

Metherate R. 2004. Nicotinic acetylcholine receptors in sensory cortex. Learn Mem 11:50–59.

Metherate R. 2011. Functional connectivity and cholinergic modulation in auditory cortex. Neurosci Biobehav Rev 35:2058–2063.

Metherate R, Hsieh CY. 2004. Synaptic mechanisms and cholinergic regulation in auditory cortex. Prog Brain Res 145:143–156.

Micu I, Ridsdale A, Zhang L, Woulfe J, McClintock J, Brantner CA, Andrews SB, Stys PK. 2007. Real-time measurement of free Ca2+ changes in CNS myelin by two-photon microscopy. Nat Med 13: 874–879.

Mitchell JB, Lupica CR, Dunwiddie TV. 1993. Activity-dependent release of endogenous adenosine modulates synaptic responses in the rat hippocampus. J Neurosci 13:3439–3447.

Moriguchi S, Mizoguchi Y, Tomimatsu Y, Hayashi Y, Kadowaki T, Kagamiishi Y, Katsube N, Yamamoto K, Inoue K, Watanabe S, et al. 2003. Potentiation of NMDA receptor-mediated synaptic responses by microglia. Brain Res Mol Brain Res 119:160–169.

Morris GP, Clark IA, Zinn R, Vissel B. 2013. Microglia: a new frontier for synaptic plasticity, learning and memory, and neurodegenerative disease research. Neurobiol Learn Mem 105:40–53.

Muller C, Bauer NM, Schafer I, White R. 2013. Making myelin basic protein -from mRNA transport to localized translation. Front Cell Neurosci 7:169.

Navarrete M, Perea G, Fernandez de Sevilla D, Gomez-Gonzalo M, Nunez A, Martin ED, Araque A. 2012. Astrocytes mediate in vivo cholinergic-induced synaptic plasticity. PLoS Biol 10:e1001259.

Nicchia GP, Nico B, Camassa LM, Mola MG, Loh N, Dermietzel R, Spray DC, Svelto M, Frigeri A. 2004. The role of aquaporin-4 in the blood-brain barrier development and integrity: studies in animal and cell culture models. Neuroscience 129:935–945.

Oberheim NA, Wang X, Goldman S, Nedergaard M. 2006. Astrocytic complexity distinguishes the human brain. Trends Neurosci 29: 547–553.

Ochiishi T, Chen L, Yukawa A, Saitoh Y, Sekino Y, Arai T, Nakata H, Miyamoto H. 1999. Cellular localization of adenosine A1 receptors in rat forebrain: immunohistochemical analysis using adenosine A1 receptor-specific monoclonal antibody. J Comp Neurol 411:301–316.

Oswald AM, Reyes AD. 2008. Maturation of intrinsic and synaptic properties of layer 2/3 pyramidal neurons in mouse auditory cortex. J Neurophysiol 99:2998–3008.

Oswald AM, Reyes AD. 2011. Development of inhibitory timescales in auditory cortex. Cereb Cortex 21:1351–1361.

Ota Y, Zanetti AT, Hallock RM. 2013. The role of astrocytes in the regulation of synaptic plasticity and memory formation. Neural Plast 2013:185463.

Papadopoulos MC, Verkman AS. 2013. Aquaporin water channels in the nervous system. Nat Rev Neurosci 14:265–277.

Parpura V, Zorec R. 2010. Gliotransmission: exocytotic release from astrocytes. Brain Res Rev 63:83–92.

Pascual O, Casper KB, Kubera C, Zhang J, Revilla-Sanchez R, Sul JY, Takano H, Moss SJ, McCarthy K, Haydon PG. 2005. Astrocytic purinergic signaling coordinates synaptic networks. Science 310:113–116.

Pedata F, Dettori I, Coppi E, Melani A, Fusco I, Corradetti R, Pugliese AM. 2016. Purinergic signalling in brain ischemia. Neuropharmacology 104:105–130.

Pelligrino DA, Vetri F, Xu HL. 2011. Purinergic mechanisms in gliovascular coupling. Semin Cell Dev Biol 22:229–236.

Perea G, Sur M, Araque A. 2014. Neuron-glia networks: integral gear of brain function. Front Cell Neurosci 8:378.

Pocock JM, Kettenmann H. 2007. Neurotransmitter receptors on microglia. Trends Neurosci 30:527–535.

Poon MM, Choi SH, Jamieson CA, Geschwind DH, Martin KC. 2006. Identification of process-localized mRNAs from cultured rodent hippocampal neurons. J Neurosci 26:13390–13399.

Proctor WR, Dunwiddie TV. 1987. Pre- and postsynaptic actions of adenosine in the in vitro rat hippocampus. Brain Res 426:187–190.

Rebola N, Pinheiro PC, Oliveira CR, Malva JO, Cunha RA. 2003. Subcellular localization of adenosine A(1) receptors in nerve terminals and synapses of the rat hippocampus. Brain Res 987:49–58.

Rebola N, Rodrigues RJ, Lopes LV, Richardson PJ, Oliveira CR, Cunha RA. 2005. Adenosine A1 and A2A receptors are co-expressed in pyramidal neurons and co-localized in glutamatergic nerve terminals of the rat hippocampus. Neuroscience 133: 79–83.

Recanzone GH, Schreiner CE, Merzenich MM. 1993. Plasticity in the frequency representation of primary auditory cortex following discrimination training in adult owl monkeys. J Neurosci 13:87–103.

Rivkees SA. 1995. The ontogeny of cardiac and neural A1 adenosine receptor expression in rats. Brain Res Dev Brain Res 89:202–213.

Rivkees SA, Price SL, Zhou FC. 1995. Immunohistochemical detection of A1 adenosine receptors in rat brain with emphasis on localization in the hippocampal formation, cerebral cortex, cerebellum, and basal ganglia. Brain Res 677:193–203.

Rombo DM, Dias RB, Duarte ST, Ribeiro JA, Lamsa KP, Sebastiao AM. 2016. Adenosine A1 receptor suppresses tonic GABAA receptor currents in hippocampal pyramidal cells and in a defined subpopulation of interneurons. Cereb Cortex 26: 1081–1095.

Saadoun S, Papadopoulos MC, Watanabe H, Yan D, Manley GT, Verkman AS. 2005. Involvement of aquaporin-4 in astroglial cell migration and glial scar formation. J Cell Sci 118:5691–5698.

Sakers K, Lake AM, Khazanchi R, Ouwenga R, Vasek MJ, Dani A, Dougherty JD. 2017. Astrocytes locally translate transcripts in their peripheral processes. Proc Natl Acad Sci U S A 114: E3830–E3838.

Sanes DH, Bao S. 2009. Tuning up the developing auditory CNS. Curr Opin Neurobiol 19:188–199.

Sanes DH, Woolley SM. 2011. A behavioral framework to guide research on central auditory development and plasticity. Neuron 72:912–929.

Sarro EC, von Trapp G, Mowery TM, Kotak VC, Sanes DH. 2015. Cortical synaptic inhibition declines during auditory learning. J Neurosci 35:6318–6325.

Schreiner CE, Polley DB. 2014. Auditory map plasticity: diversity in causes and consequences. Curr Opin Neurobiol 24:143–156.

Sebastiao AM, Ribeiro JA. 2009. Tuning and fine-tuning of synapses with adenosine. Curr Neuropharmacol 7:180–194.

Sebastiao AM, Ribeiro JA. 2015. Neuromodulation and metamodulation by adenosine: Impact and subtleties upon synaptic plasticity regulation. Brain Res 1621:102–113.

Shiota C, Miura M, Mikoshiba K. 1989. Developmental profile and differential localization of mRNAs of myelin proteins (MBP and PLP) in oligodendrocytes in the brain and in culture. Brain Res Dev Brain Res 45:83–94.

Smith AJ, Jin BJ, Ratelade J, Verkman AS. 2014. Aggregation state determines the localization and function of M1- and M23-aquaporin-4 in astrocytes. J Cell Biol 204:559–573.

Sperlagh B, Vizi ES. 2011. The role of extracellular adenosine in chemical neurotransmission in the hippocampus and Basal Ganglia: pharmacological and clinical aspects. Curr Top Med Chem 11:1034–1046.

Stevens B, Porta S, Haak LL, Gallo V, Fields RD. 2002. Adenosine: a neuron-glial transmitter promoting myelination in the CNS in response to action potentials. Neuron 36:855–868.

Steward O, Levy WB. 1982. Preferential localization of polyribosomes under the base of dendritic spines in granule cells of the dentate gyrus. J Neurosci 2:284–291.

Storace DA, Higgins NC, Chikar JA, Oliver DL, Read HL. 2012. Gene expression identifies distinct ascending glutamatergic pathways to frequency-organized auditory cortex in the rat brain. J Neurosci 32:15759–15768.

Swanson TH, Drazba JA, Rivkees SA. 1995. Adenosine A1 receptors are located predominantly on axons in the rat hippocampal formation. J Comp Neurol 363:517–531.

Takesian AE, Hensch TK. 2013. Balancing plasticity/stability across brain development. Prog Brain Res 207:3–34.

Tetzlaff W, Schubert P, Kreutzberg GW. 1987. Synaptic and extrasynaptic localization of adenosine binding sites in the rat hippocampus. Neuroscience 21:869–875.

Tiruchinapalli DM, Oleynikov Y, Kelic S, Shenoy SM, Hartley A, Stanton PK, Singer RH, Bassell GJ. 2003. Activity-dependent trafficking and dynamic localization of zipcode binding protein 1 and beta-actin mRNA in dendrites and spines of hippocampal neurons. J Neurosci 23:3251–3261.

Trapp BD, Moench T, Pulley M, Barbosa E, Tennekoon G, Griffin J. 1987. Spatial segregation of mRNA encoding myelin-specific proteins. Proc Natl Acad Sci U S A 84:7773–7777.

Tremblay ME, Majewska AK. 2011. A role for microglia in synaptic plasticity? Commun Integr Biol 4:220–222.

Tremblay ME, Lowery RL, Majewska AK. 2010. Microglial interactions with synapses are modulated by visual experience. PLoS Biol 8:e1000527.

Tremblay ME, Zettel ML, Ison JR, Allen PD, Majewska AK. 2012. Effects of aging and sensory loss on glial cells in mouse visual and auditory cortices. GLIA 60:541–558.

Tsutsui S, Schnermann J, Noorbakhsh F, Henry S, Yong VW, Winston BW, Warren K, Power C. 2004. A1 adenosine receptor upregulation and activation attenuates neuroinflammation and demyelination in a model of multiple sclerosis. J Neurosci 24: 1521–1529.

Turtzo LC, Lescher J, Janes L, Dean DD, Budde MD, Frank JA. 2014. Macrophagic and microglial responses after focal traumatic brain injury in the female rat. J Neuroinflammation 11:82.

Venero JL, Vizuete ML, Ilundain AA, Machado A, Echevarria M, Cano J. 1999. Detailed localization of aquaporin-4 messenger RNA in the CNS: preferential expression in periventricular organs. Neuroscience 94:239–250.

Verity AN, Campagnoni AT. 1988. Regional expression of myelin protein genes in the developing mouse brain: in situ hybridization studies. J Neurosci Res 21:238–248.

Vindeirinho J, Costa GN, Correia MB, Cavadas C, Santos PF. 2013. Effect of diabetes/hyperglycemia on the rat retinal adenosinergic system. PLoS One 8:e67499.

Vogel C, Marcotte EM. 2012. Insights into the regulation of protein abundance from proteomic and transcriptomic analyses. Nat Rev Genet 13:227–232.

Wake H, Moorhouse AJ, Jinno S, Kohsaka S, Nabekura J. 2009. Resting microglia directly monitor the functional state of synapses in vivo and determine the fate of ischemic terminals. J Neurosci 29:3974–3980.

Wake H, Moorhouse AJ, Miyamoto A, Nabekura J. 2013. Microglia: actively surveying and shaping neuronal circuit structure and function. Trends Neurosci 36:209–217.

Wall M, Dale N. 2008. Activity-dependent release of adenosine: a critical re-evaluation of mechanism. Curr Neuropharmacol 6: 329–337.

Wall MJ, Dale N. 2013. Neuronal transporter and astrocytic ATP exocytosis underlie activity-dependent adenosine release in the hippocampus. J Physiol 591:3853–3871.

Wang X, Lou N, Xu Q, Tian GF, Peng WG, Han X, Kang J, Takano T, Nedergaard M. 2006. Astrocytic Ca2+ signaling evoked by sensory stimulation in vivo. Nat Neurosci 9:816–823.

Wang F, Flanagan J, Su N, Wang LC, Bui S, Nielson A, Wu X, Vo HT, Ma XJ, Luo Y. 2012. RNAscope: a novel in situ RNA analysis platform for formalin-fixed, paraffin-embedded tissues. J Mol Diagn 14:22–29.

Watson C, Paxinos G, Puelles L, editors. 2012. *The mouse nervous system*. London, UK: Academic Press.

Wei CJ, Li W, Chen JF. 2011. Normal and abnormal functions of adenosine receptors in the central nervous system revealed by genetic knockout studies. Biochim Biophys Acta 1808:1358–1379.

Weinberger NM. 2004. Specific long-term memory traces in primary auditory cortex. Nat Rev Neurosci 5:279–290.

Weinberger NM. 2007. Auditory associative memory and representational plasticity in the primary auditory cortex. Hear Res 229: 54–68.

Wetherington JP, Lambert NA. 2002. Differential desensitization of responses mediated by presynaptic and postsynaptic A1 adenosine receptors. J Neurosci 22:1248–1255.

Wimmer VC, Broser PJ, Kuner T, Bruno RM. 2010. Experience-induced plasticity of thalamocortical axons in both juveniles and adults. J Comp Neurol 518:4629–4648.

Winer JA. 2005. Decoding the auditory corticofugal systems. Hear Res 207:1–9.

Winer JA, Larue DT. 1996. Evolution of GABAergic circuitry in the mammalian medial geniculate body. Proc Natl Acad Sci U S A 93: 3083–3087.

Winship IR, Plaa N, Murphy TH. 2007. Rapid astrocyte calcium signals correlate with neuronal activity and onset of the hemodynamic response in vivo. J Neurosci 27:6268–6272.

Yamaguchi D, Terayama R, Omura S, Tsuchiya H, Sato T, Ichikawa H, Sugimoto T. 2014. Effect of adenosine A1 receptor agonist on the enhanced excitability of spinal dorsal horn neurons after peripheral nerve injury. Int J Neurosci 124:213–222.

Yuge K, Kataoka A, Yoshida AC, Itoh D, Aggarwal M, Mori S, Blackshaw S, Shimogori T. 2011. Region-specific gene expression in early postnatal mouse thalamus. J Comp Neurol 519:544–561.

Zeisel A, Munoz-Manchado AB, Codeluppi S, Lonnerberg P, La Manno G, Jureus A, Marques S, Munguba H, He L, Betsholtz C, et al. 2015. Brain structure. Cell types in the mouse cortex and hippocampus revealed by single-cell RNA-seq. Science 347: 1138–1142.

Zhang LI, Poo MM. 2001. Electrical activity and development of neural circuits. Nat Neurosci 4(Suppl):1207–1214.

Zhang LI, Bao S, Merzenich MM. 2001. Persistent and specific influences of early acoustic environments on primary auditory cortex. Nat Neurosci 4:1123–1130.

Zhang JM, Wang HK, Ye CQ, Ge W, Chen Y, Jiang ZL, Wu CP, Poo MM, Duan S. 2003. ATP released by astrocytes mediates glutamatergic activity-dependent heterosynaptic suppression. Neuron 40:971–982.

Zhang Y, Chen K, Sloan SA, Bennett ML, Scholze AR, O'Keeffe S, Phatnani HP, Guarnieri P, Caneda C, Ruderisch N, et al. 2014. An RNA-sequencing transcriptome and splicing database of glia, neurons, and vascular cells of the cerebral cortex. J Neurosci 34: 11929–11947.

Zhong J, Zhang T, Bloch LM. 2006. Dendritic mRNAs encode diversified functionalities in hippocampal pyramidal neurons. BMC Neurosci 7:17.

Zhu ZR, Xu F, Ji WG, Ren SC, Chen F, Chen PZ, Jiang HH, Mi Z, Hu B, Zhang J, et al. 2014. Synaptic mechanisms underlying thalamic activation-induced plasticity in the rat auditory cortex. J Neurophysiol 111:1746–1758.

Zimmermann H. 2011. Purinergic signaling in neural development. Semin Cell Dev Biol 22:194–204.

Zimmermann H, Zebisch M, Strater N. 2012. Cellular function and molecular structure of ecto-nucleotidases. Purinergic Signal 8: 437–502.